For Reference

NOT TO BE TAKEN FROM THIS ROOM

For Reference

NOT TO BE TAKEN FROM THIS ROOM

Ex libris
universitatis
albertaensis

UNIVERSITY OF ALBERTA
LIBRARY

Regulations Regarding Theses and Dissertations

Typescript copies of theses and dissertations for Master's and Doctor's degrees deposited in the University of Alberta Library, as the official Copy of the Faculty of Graduate Studies, may be consulted in the Reference Reading Room only.

A second copy is on deposit in the Department under whose supervision the work was done. Some Departments are willing to loan their copy to libraries, through the inter-library loan service of the University of Alberta Library.

These theses and dissertations are to be used only with due regard to the rights of the author. Written permission of the author and of the Department must be obtained through the University of Alberta Library when extended passages are copied. When permission has been granted, acknowledgement must appear in the published work.

This thesis or dissertation has been used in accordance with the above regulations by the persons listed below. The borrowing library is obligated to secure the signature of each user.

Please sign below:

Date	Signature	Institution

THE UNIVERSITY OF ALBERTA

MOMENT CURVATURE RELATIONSHIPS OF PRESTRESSED CONCRETE BEAMS WITH CONFINED COMPRESSED CONCRETE

by

MALCOLM KEITH WILKINSON

A THESIS

SUBMITTED TO THE FACULTY OF GRADUATE STUDIES

IN PARTIAL FULFILMENT OF THE REQUIREMENTS FOR THE DEGREE

OF MASTER OF SCIENCE

DEPARTMENT OF CIVIL ENGINEERING

EDMONTON, ALBERTA

SPRING, 1980

THE UNIVERSITY OF ALBERTA

MOMENT CURVATURE RELATIONSHIPS OF PRESTRESSED CONCRETE BEAMS WITH CONFINED COMPRESSED CONCRETE

by

© MALCOLM KEITH WILKINSON

A THESIS

SUBMITTED TO THE FACULTY OF GRADUATE STUDIES

IN PARTIAL FULFILMENT OF THE REQUIREMENTS FOR THE DEGREE

OF MASTER OF SCIENCE

DEPARTMENT OF CIVIL ENGINEERING

EDMONTON, ALBERTA

SPRING, 1969

THE UNIVERSITY OF ALBERTA

MOMENT CURVATURE RELATIONSHIPS OF PRESTRESSED CONCRETE BEAMS WITH CONFINED COMPRESSED CONCRETE

by

© MALCOLM KEITH WILKINSON

A THESIS

SUBMITTED TO THE FACULTY OF GRADUATE STUDIES

IN PARTIAL FULFILLMENT OF THE REQUIREMENTS FOR THE DEGREE

OF MASTER OF SCIENCE

DEPARTMENT OF CIVIL ENGINEERING

EDMONTON, ALBERTA

SPRING, 1969

1969
143

UNIVERSITY OF ALBERTA

FACULTY OF GRADUATE STUDIES

The undersigned certify that they have read, and recommend to the Faculty of Graduate Studies for acceptance, a thesis entitled MOMENT CURVATURE RELATIONSHIPS OF PRESTRESSED CONCRETE BEAMS WITH CONFINED COMPRESSED CONCRETE submitted by MALCOLM KEITH WILKINSON in partial fulfilment of the requirements for the degree of Master of Science.

Date Dec 11 1968

UNIVERSITY OF ALBERTA

FACULTY OF GRADUATE STUDIES

The undersigned certify that they have read, and recommend to the Faculty of Graduate Studies for acceptance, a thesis entitled MOMENT CURVATURE RELATIONSHIPS OF PRESTRESSED CONCRETE BEAMS WITH CONFINED COMPRESSED CONCRETE submitted by MALCOLM KEITH WILKINSON in partial fulfillment of the requirements for the degree of Master

ABSTRACT

The object of this investigation was to study the behaviour, and failure modes of bonded prestressed concrete beams, with confined compressed concrete, subjected to a moment gradient. The confinement was achieved using 6-in. outside diameter spiral-wound reinforcement in the concrete compression zone of the prestressed beams. The effects of the variables such as amount of tension reinforcement, beam span, and spiral pitch on the moment-curvature relationships, and their influence on the types of failure modes were studied.

Twelve beams having a nominal 6-in. by 14-5/8 in. cross-section and an effective depth of 10-in. were loaded with a single concentrated load applied at mid-span. The beams were simply supported. Six beams were tested using a 10-ft. span and six using a 5-ft. span. The beams were classified as "normally over-reinforced in tension" according to the ACI STANDARD 318-63 Building Code Requirements for Reinforced Concrete. The behaviour of the test beams is presented in terms of the measured load-deflection relationships and the derived moment-curvature relationships.

The confined compression concrete zone improved the ductility and rotation capacity to such an extent that a beam could resist its maximum applied moment over a large range of mid-span curvature until ultimate failure. Where sufficient confinement had been provided, ductile tension type failures occurred even though the beams would be normally considered over-reinforced in tension.

ACKNOWLEDGEMENTS

This investigation is part of a continuing experimental program, supervised by Dr. J. Warwaruk*, to study the effect of confined compressed concrete in prestressed concrete beams. The investigation was made possible through funds and facilities provided by the Department of Civil Engineering together with financial assistance given by the National Research Council of Canada.

The author wishes to express his sincere appreciation to Dr. J. Warwaruk for his guidance in planning the test series and in the preparation of the manuscript.

The author wishes to thank Messrs. H. Panse, L. Burden, R. Lindner, R. Resaul, and R. Blair, for their assistance in the fabrication of the test beams and the test program.

Miss Lynne Fiveland typed the manuscript with care and her cooperation is appreciated.

* Dr. J. Warwaruk
Associate Professor
Department of Civil Engineering
University of Alberta.

TABLE OF CONTENTS

		PAGE
Title Page		i
Approval Sheet		ii
Abstract		iii
Acknowledgements		iv
Table of Contents		v
List of Tables		vi
List of Figures		vii
CHAPTER I	INTRODUCTION	1
CHAPTER II	PREVIOUS TESTS	3
CHAPTER III	PRESENT TEST SERIES	10
CHAPTER IV	TEST RESULTS	23
CHAPTER V	DISCUSSION OF TEST RESULTS	39
CHAPTER VI	SUMMARY, CONCLUSIONS, AND RECOMMENDATIONS	52
LIST OF REFERENCES		55
NOTATION		56
APPENDIX	MATERIALS, FABRICATION, PRESTRESS LOSS AND LOADING APPARATUS	57

LIST OF TABLES

PAGE

TABLE 2.1 A Summary of the Test Results of Raffa (2) 8

TABLE 2.2 A Summary of the Test Results of Belke (3) 9

TABLE 3.1 Details of Test Beams 15

TABLE 5.1 A Comparison of Mid-Span Curvatures 47

TABLE 5.2 A Summary of the Test Results 48

TABLE A.1 Sieve Analysis of Sand 64

TABLE A.2 Sieve Analysis of Coarse Aggregate 64

TABLE A.3 Concrete Cylinder Strengths and Properties 65

TABLE A.4 Concrete Design Properties 66

TABLE A.5 Prestress Losses and Effective Prestress 67

LIST OF FIGURES

		PAGE
FIGURE 3.1	Test Beam Cross-Sections	16
FIGURE 3.2	Shear Reinforcement Series 'D' and 'E' Beams . .	17
FIGURE 3.3	Shear Reinforcement Series 'F' and 'G' Beams . .	18
FIGURE 3.4	Instrumentation Series 'D' and 'F' Beams	19
FIGURE 3.5	Instrumentation Series 'E' and 'G' Beams	20
FIGURE 3.6	Strain Gauges on the Spiral Reinforcement . . .	21
FIGURE 3.7	Arrangement of Dial Gauges for Beam F1	22
FIGURE 3.8	Beam F1 Prepared for Testing	22
FIGURE 4.1	Measured Load v. Mid-span Deflection Beam F1 . .	26
FIGURE 4.2	M/M_i v. Mid-span Curvature Beam F1	26
FIGURE 4.3	Strain Distributions along Beam F1	27
FIGURE 4.4	M/M_i v. Spiral Reinforcement Strains Beam F1 . .	28
FIGURE 4.5	Measured Load v. Mid-span Deflection Diagrams Series 'D' and 'F' Beams	29
FIGURE 4.6	Measured Load v. Mid-span Deflection Diagrams Series 'E' and 'G' Beams	30
FIGURE 4.7	Strain Distribution at Top Compression Fibre Series 'D' and 'F' Beams	31
FIGURE 4.8	Strain Distribution at Top Compression Fibre Series 'E' and 'G' Beams	32
FIGURE 4.9	M/M_i v. Mid-span Curvature Series 'D' and 'F' Beams	33

PAGE

FIGURE 4.10 M/M_i v. Mid-span Curvature Series 'E' and 'G' Beams 34

FIGURE 4.11 M/M_i v. Spiral Reinforcement Strains Series 'D' Beams 35

FIGURE 4.12 M/M_i v. Spiral Reinforcement Strains Series 'F' Beams 36

FIGURE 4.13 M/M_i v. Spiral Reinforcement Strains Series 'E' Beams 37

FIGURE 4.14 M/M_i v. Spiral Reinforcement Strains Series 'G' Beams 38

FIGURE 5.1 Failure Modes of Series 'D', 'E', 'F' and 'G' Beams 49

FIGURE 5.2 Spalling at the Compression Zone in Beam D1 . . . 50

FIGURE 5.3 Shear Cracks Penetrate the Compression Zone in Beam E1 50

FIGURE 5.4 Arching Between Spiral Loops in Beam D2 50

FIGURE 5.5 Arching Between Spiral Loops in Beam F3 50

FIGURE 5.6 Tension Failure of Spiral Steel in Beam G2 . . . 51

FIGURE 5.7 Shear Cracks and Rupture of the Compression Zone in Beam G2 51

FIGURE 5.8 Compression Failure in Beam E3 51

FIGURE 5.9 Crack Patterns at Initial Crushing in Beam F2 51

PAGE

FIGURE A.1	Stress-Strain Diagram for Prestressing Strand . .	68
FIGURE A.2	Stress-Strain Diagram for Spiral Reinforcement. .	69
FIGURE A.3	Erected Beam Forms	70
FIGURE A.4	Simplex Hydraulic Jack and Grip Assembly at South Bulkhead	70
FIGURE A.5	Aluminum Dynamometers and Strain Indicator at North Bulkhead	70
FIGURE A.6	Prestressing Equipment	70
FIGURE A.7	Shear Stirrups Wired to Prestressed Cables . . .	71
FIGURE A.8	Loading Frame	71

CHAPTER I

INTRODUCTION

A limit analysis design procedure of prestressed concrete beams requires a sound knowledge of the inelastic behaviour of these beams. Inelastic behaviour is limited by the amount of deformation which can occur at critical sections when the prestressed beams are subjected to applied loads. Moment-curvature relationships are a convenient way of representing the inelastic behaviour as they relate the resisting moments to the deformations which occur at a section. In normal prestressed concrete beams the reinforcement has limited ductility and the curvature may not be sufficient to permit limit analysis. Additional curvature can be obtained by confining the concrete compression zone using a continuous spiral reinforcement. For the spiral to be effective, it is also necessary to increase the amount of tension reinforcement from that in normal prestressed concrete beams. Such beams are capable of exhibiting large curvatures.

The object of this investigation is to study the behaviour of a series of twelve rectangular prestressed concrete beams with confined compressed concrete, subjected to a moment gradient. The concrete compression zone is laterally confined with spiral-wound reinforcement at the maximum moment region at mid-span. The degree of confinement is varied to determine the effect of the amount of confinement on the moment-curvature relationships, and the amount of confinement necessary to maintain ductility in the beams.

The investigation includes tests on twelve prestressed concrete beams with confined compressed concrete. The major variables in the tests are the degree of confinement, the amount of tension reinforcement, and the beam span. There are small variations in the effective prestress levels, and nominal variations in the concrete strengths. The concrete strength was increased when it was observed that in some tests the extent of the deformations was limited by the shear resistance of the beams. A detailed outline of the test beams and variables is presented in Chapter III. A discussion of the behaviour is presented in Chapter V and brief comparisons are made with previous tests on similar beams without confined compressed concrete.

CHAPTER II

REVIEW OF PREVIOUS TESTS

The concept of a limit analysis procedure applied to prestressed concrete beams has resulted in extensive experimental investigations of the behaviour characteristics of these beams. Limit analysis requires that the beams possess sufficient rotation capacity to permit plastic hinges to form at critical sections. For prestressed beams, the rotations required can be obtained from deformations both in the concrete and the reinforcement. Only a limited rotation capacity is available from the reinforcement since it has a limited ductility and some of the available deformation has been lost due to prestressing. The additional rotation capacity must be obtained from deformations in the concrete compression zone prior to the failure of the tension reinforcement.

According to the ACI Building Code (5), beams are normally classified as over-reinforced or under-reinforced depending on the relative amount of reinforcement with respect to concrete. Under-reinforced beams are those which exhibit a large ductility or deformation prior to failure. The normally under-reinforced prestressed beam, according to the ACI Building Code, is ductile, but it does not posses very much rotation capacity. To increase the rotation capacity it is necessary to ensure that the strains in the reinforcement remain below the failure strain while the increased additional rotation capacity occurs in the concrete. Since the compressed concrete by itself can sustain

strains of the order of 0.004 to 0.006 prior to crushing, it is necessary to provide a means by which the concrete can develop higher strains. This is possible by confining the concrete.

Spiral reinforcement is used to confine the concrete in bound concrete columns to promote ductile failures and develop a reserve strength. Similarly, this technique may be used in beams. By lateral confinement of the compression zone concrete, the ductility and the rotation capacity of a prestressed beam are increased. The confined compression zone permits a portion of the beam to remain intact, and as the load is maintained, or increased, the reinforcement itself yields. The beam finally fails in a ductile manner even though the amount of reinforcement present would normally classify the beam as over-reinforced.

Tests carried out at the University of Alberta (2), (3), (4), present the behaviour of prestressed beams in terms of load-deflection and moment-curvature relationships. Information regarding the distribution of curvature is also presented. Similar information is available in references (1), (6) and (7).

Raffa (2) studied the deformation characteristics of bonded prestressed beams, without confinement, loaded in flexure and shear. The moment-curvature relationships were calculated from measured strains and deflections, and compared with the computed relationships. The relationships depended on the material properties of the beams and were affected by:-

(1) cracking of the concrete,

(2) changes from elastic to inelastic behaviour,

(3) the level of prestress,

(4) the concrete strength, and

(5) the span length.

The relationships exhibited three behaviour stages which corresponded to:-

(1) elastic strains in the concrete and reinforcement,

(2) elastic strains in the reinforcement while the concrete strains changed from elastic to inelastic,

(3) inelastic strains in both reinforcement and concrete.

Maximum strains occurred at mid-span over the entire loading range. Large deflections which were recorded after initial crushing of the concrete were influenced by:-

(1) the confining effect of the load bearing plate at mid-span,

(2) the transfer of stresses to adjacent less strained sections of the beams as crushing developed, and

(3) the spacing of the shear stirrups.

The beams failed ultimately by tension failure of the prestressed reinforcement. A summary of the details of the test results are presented in Table 2.1.

Belke (3) also studied the deformation characteristics of bonded prestressed beams, without confinement, loaded in flexure and shear. Measured and theoretical moment-curvature relationships were presented and compared. The measured load-deflection relationships were compared with those computed from the measured curvature distributions.

The relationships depended on the properties of the beam cross-section and span length, and the three distinct behaviour stages reported by Raffa were exhibited. Belke concluded:-

(1) for constant f_c' and span length,

(a) the change in curvature for an increment of applied moment was reduced for an increased amount of tension reinforcement,

(b) a greater percentage of reinforcement increased the beam stiffness more effectively in the beams with higher concrete strengths,

(2) for increased f_c', a larger moment was required to produce a given deformation.

A summary of the details of these tests is presented in Table 2.2.

Ward (4) tested a series of prestressed concrete beams loaded in flexure, with spiral reinforcement in the concrete compression zone, to study the effects of lateral confinement of the compression zone on the load-deflection and moment-curvature relationships. The influence of the type and amount of confinement was studied by varying the diameter and pitch of the spiral reinforcement. The moment-curvature and load-deflection relationships were determined. The theoretically derived moment-curvature relationships, calculated at loads prior to spalling and assuming no spiral influence, were compared to those computed from the measured strain distributions. A further stage in the behaviour was observed, commencing with spalling of the concrete compression zone. The strains in the tension reinforcement which had

remained elastic to this stage, became inelastic because of a sudden drop in beam stiffness and the redistribution of stresses as the concrete was restrained by the lateral reinforcement. Ward concluded:-

(1) lateral confinement of the compression zone concrete was effective in producing ductile failures in normally over-reinforced prestressed concrete beams,

(2) smaller reduction in beam stiffness occurred in the case of two small overlapping spirals than for a single large diameter spiral,

(3) compression failures occurred either by yielding of the spiral reinforcement or by concrete arch failure, and

(4) the ultimate moment and curvature of beams with a high degree of confinement depended mainly on the amount of tension reinforcement.

TABLE 2.1

A SUMMARY OF THE TEST RESULTS OF RAFFA (2)

Beam	Span	f_c' (psi)	A_s (in^2)	$p = \frac{A_s}{bd}$	Effective Prestress (ksi)	Type of Failure	Observed M_u (kip-ft)	Observed M_{CR} (kip-ft)	Shear Reinforcement	P_u (approx) (kip)	Δ_{MAX} (approx) (ins)
7	11'-0"	7550	0.2308	0.00384	133	TENSION	49.0	22.0	#2 @ 6"	18.0	2.2
8	11'-0"	5380	0.2308	0.00384	133	TENSION	48.0	22.0	#2 @ 6"	17.5	2.5
9	4'-8"	6200	0.2308	0.00384	134	TENSION	50.0	22.5	#2 @ 3"	43.0	1.4
10	4'-8"	4280	0.2308	0.00384	133	TENSION	48.0	21.0	#2 @ 3"	41.0	1.3

TABLE 2.2

A SUMMARY OF THE TEST RESULTS OF BELKE (3)

Beam	Span	f_c' (psi)	A_s (in^2)	$p = \frac{A_s}{bd}$	Effective Prestress (ksi)	Type of Failure	Observed M_u (kip-ft)	Observed M_{CR} (kip-ft)	Shear Reinforcement	P_u (approx) (kip)	Δ_{MAX} (approx) (ins)
2A	11'-0"	3450	0.3468	0.00578	138	COMPRESSION	60.5	30.2	#2 @ 6"	21.5	1.10
3A	11'-0"	3550	0.4624	0.00770	130	COMPRESSION	67.0	41.0	#3 @ 6"	26.0	0.83
5A	11'-0"	6840	0.3468	0.00578	142	COMPRESSION	74.8	34.4	#2 @ 5"	26.0	1.75
6A	11'-0"	6890	0.4624	0.00770	144	COMPRESSION	96.3	44.0	#3 @ 5"	34.0	1.00
2B	5'-6"	4250	0.3468	0.00578	136	COMPRESSION	68.7	35.7	#3 @ 2-1/2"	50.0	0.42
3B	5'-6"	3550	0.4624	0.00770	137	COMPRESSION	75.6	44.0	#3 @ 2"	56.0	0.45
5B	5'-6"	6460	0.3468	0.00578	143	BOND	71.5	36.3	#3 @ 2-1/2"	51.0	0.50
6B	5'-6"	5940	0.4624	0.00770	144	BOND	83.6	44.5	#3 @ 2"	59.0	0.50

CHAPTER III

PRESENT TEST SERIES

The present test series was conducted to compare the behaviour of prestressed concrete beams with confined compression concrete, subject to bending and shear, to the behaviour of similar beams without confinement (3). This chapter presents an outline of the test program, the instrumentation and design of the test beams, and a description of the test procedure. Further details of the geometrical and material properties of the beams, fabrication, prestress losses, and loading apparatus are presented in the Appendix.

OUTLINE

Twelve beams consisting of four series of three beams were tested with the following as main variables:-

(1) amount of tension reinforcement,

(2) beam span, and

(3) degree of confinement of the concrete compression zone.

The four series were D, E, F and G and the specific beams in a series, eg. D, were D1, D2, and D3. The number represents the pitch, in inches, of the spiral reinforcement used to confine the concrete compression zone. Series D and F beams were tested on a 10-ft. span and series E and G on a 5-ft. span. All beams were loaded with a concentrated load at mid-span and were simply supported.

DESIGN

In this test series, the major variable is the amount of spiral reinforcement used to confine the concrete compression zone. In addition, the behaviour of the beams will be affected by the concrete strength, and the beam span for a fixed amount of tension reinforcement. The test beams were designed to determine:-

(1) the effect of the degree of confinement of the concrete compression zone for a fixed amount of tension reinforcement, similar concrete strengths, and a constant span length,

(2) the failure mode of beams with the same degree of confinement, fixed amount of tension reinforcement, similar concrete strengths, and varying span lengths,

(3) the effect of the amount of tension reinforcement for the same degree of confinement, constant span length, and similar concrete strengths, and

(4) the effect of the degree of confinement for varying concrete strengths.

The test beams were designed for a nominal concrete strength of 5,000 psi. Series D and E beams, prestressed with six cables of 7-wire strand, 5/16-in. nominal diameter, satisfied balanced design conditions according to the ACI Building Code (5). Series F and G beams, prestressed with eight cables, were over-reinforced. The beams were 6-in. by 14-5/8 in. in cross-section and had an effective depth of 10-in., as shown in Figure 3.1. A 17-in. bond transfer length, beyond the supports, was provided for series D and E beams, and it was increased

to 22-in. for series F and G beams. In each beam the concrete compression zone was confined with a 4-ft. length of 6-in. outside diameter spiral-wound reinforcement. Spiral pitches of one, two, and three inches were used in each series. The shear reinforcement used, consisted of bent stirrups designed according to the minimum requirements of the ACI Building Code (5), and is shown in Figures 3.2 and 3.3 The spiral reinforcement was assumed not to contribute to the shear carrying capacity of the concrete.

INSTRUMENTATION

The instrumentation of the beams was planned to measure the deformations and deflections from which moment-curvature relationships and distributions of curvature could be obtained. Curvatures were obtained primarily from measurements of deformations on the side of the beam using a Demec Gauge. Curvatures were calculated from deflection measurements and checked with those obtained by the Demec measurements. In the later stages of loading, curvatures were calculated from the deflection measurements. An instrumented gauge length of 6-ft. was used for series D and F beams, and 2-ft. for series E and G beams. It was assumed that all major cracking and crushing of the concrete compression zone would occur within these lengths.

Steel Demec gauge points, 1/4-in. diameter, were located on the front face of the beam, as shown in Figures 3.4 and 3.5, to determine the strain in the top compression fibre and the strain distribution over the effective beam depth. Beam deflections were measured using

dial gauges, and a precise level. The dial gauges were removed at initial failure of the extreme concrete compression fibre, and the deflections recorded with the precise level until ultimate failure. Figures 3.4 and 3.5 show the arrangement of the dial gauges and the steel rule targets for the level.

Strain measurements, on the spiral reinforcement confining the concrete compression zone, were made at three locations as shown in Figures 3.4 and 3.5. Strain gauges on the same spiral loop located eight inches from mid-span were used to determine the magnitude and strain distribution around the spiral reinforcement. At each location the concrete was chipped clear to expose a 1-1/2 in. length of the spiral reinforcement to which the strain gauges were attached.

TEST PROCEDURE

Each beam was loaded until collapse as a result of either the destruction of the confined concrete compression zone, or the fracture of the prestressed tension reinforcement. The flexural cracking load was reached within three or four load increments and the ultimate capacity reached in ten to twelve increments. The applied load increments were reduced after flexural cracking and further reduced after spalling at the extreme compression fibre. In the later loading stages, the load increments depended on the deflection and the ability of the beam to resist the load. After the application of each load increment, Demec readings, deflections, and spiral reinforcement strains were recorded, and the cracks marked. The load was maintained constant using the

automatic load maintainer of the loading apparatus. Near the predicted ultimate capacity, the load was maintained manually, and when the load dropped at spalling, it was held at the reduced value while strain and deflection measurements were recorded. Due to extensive cracking in the final loading stages, it was impossible to record the Demec readings, and only the precise level deflections and the spiral reinforcement strains were recorded. Near collapse, the deflections increased rapidly for a constant applied load, and it was only possible to record the mid-span deflection and the spiral reinforcement strains.

TABLE 3.1

DETAILS OF TEST BEAMS

Beam	Test Span (ft)	Spiral Pitch (in)	Spiral Dia. (in)	Spiral Length (ft)	f_c' (psi)	Area of Reinforcement $(in)^2$	$p = \frac{A_s}{bd}$	$\frac{p}{f_c'}$ $(10^{-7}/psi)$	Effective Prestress (ksi)
D1	10	1	6	4	3470	0.3468	0.00578	16.66	131.1
D2	10	2	6	4	3880	0.3468	0.00578	14.90	134.9
D3	10	3	6	4	3920	0.3468	0.00578	14.74	134.6
E1	5	1	6	4	3720	0.3468	0.00578	15.54	132.2
E2	5	2	6	4	4330	0.3468	0.00578	13.35	138.3
E3	5	3	6	4	3540	0.3468	0.00578	16.33	134.3
F1	10	1	6	4	5340	0.4624	0.00770	14.42	143.8
F2	10	2	6	4	5120	0.4624	0.00770	15.04	129.0
F3	10	3	6	4	3550	0.4624	0.00770	21.69	127.2
G1	5	1	6	4	5310	0.4624	0.00770	14.50	149.3
G2	5	2	6	4	4740	0.4624	0.00770	16.24	131.8
G3	5	3	6	4	3700	0.4624	0.00770	20.81	135.3

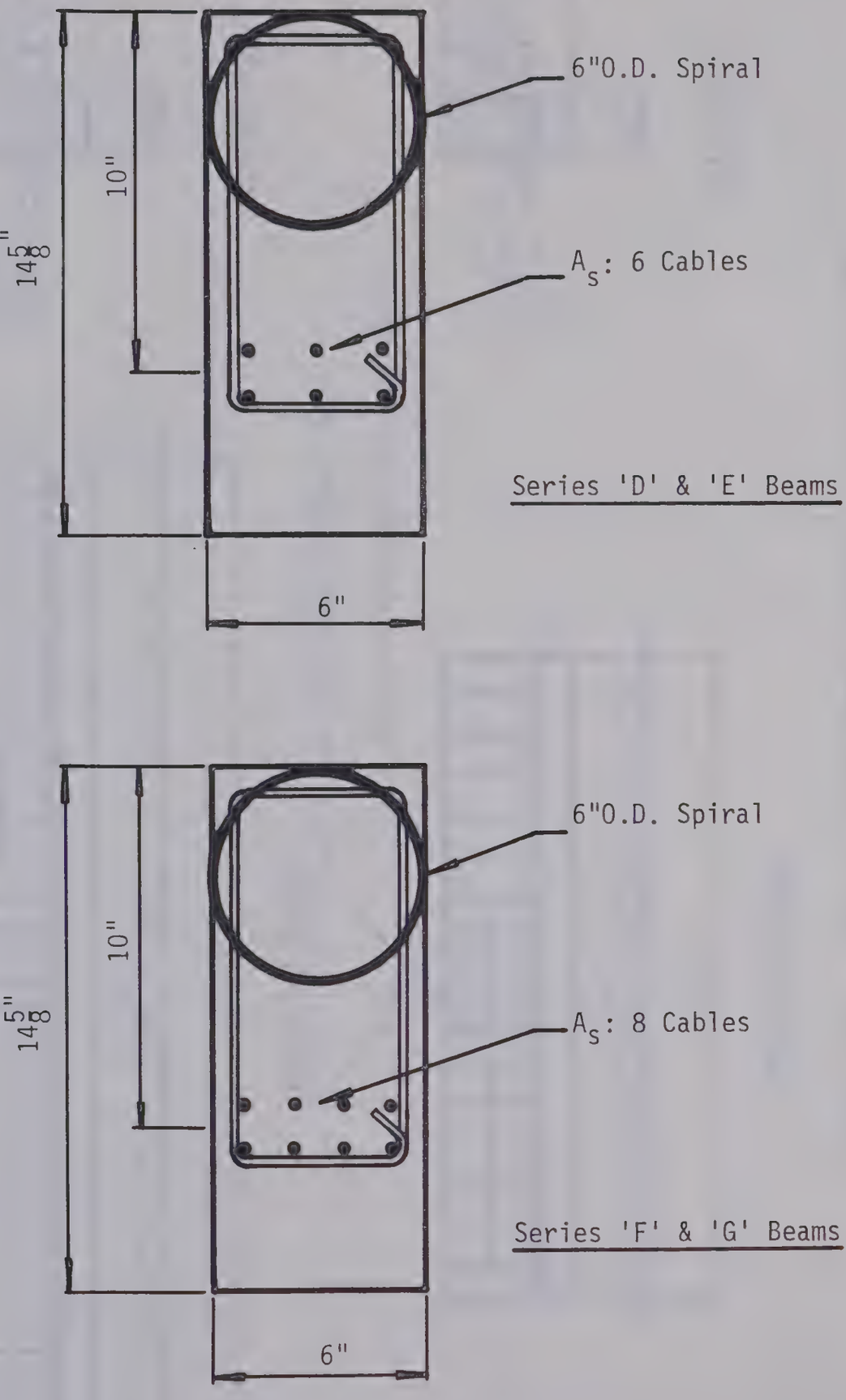

FIGURE 3.1: TEST BEAM CROSS-SECTIONS

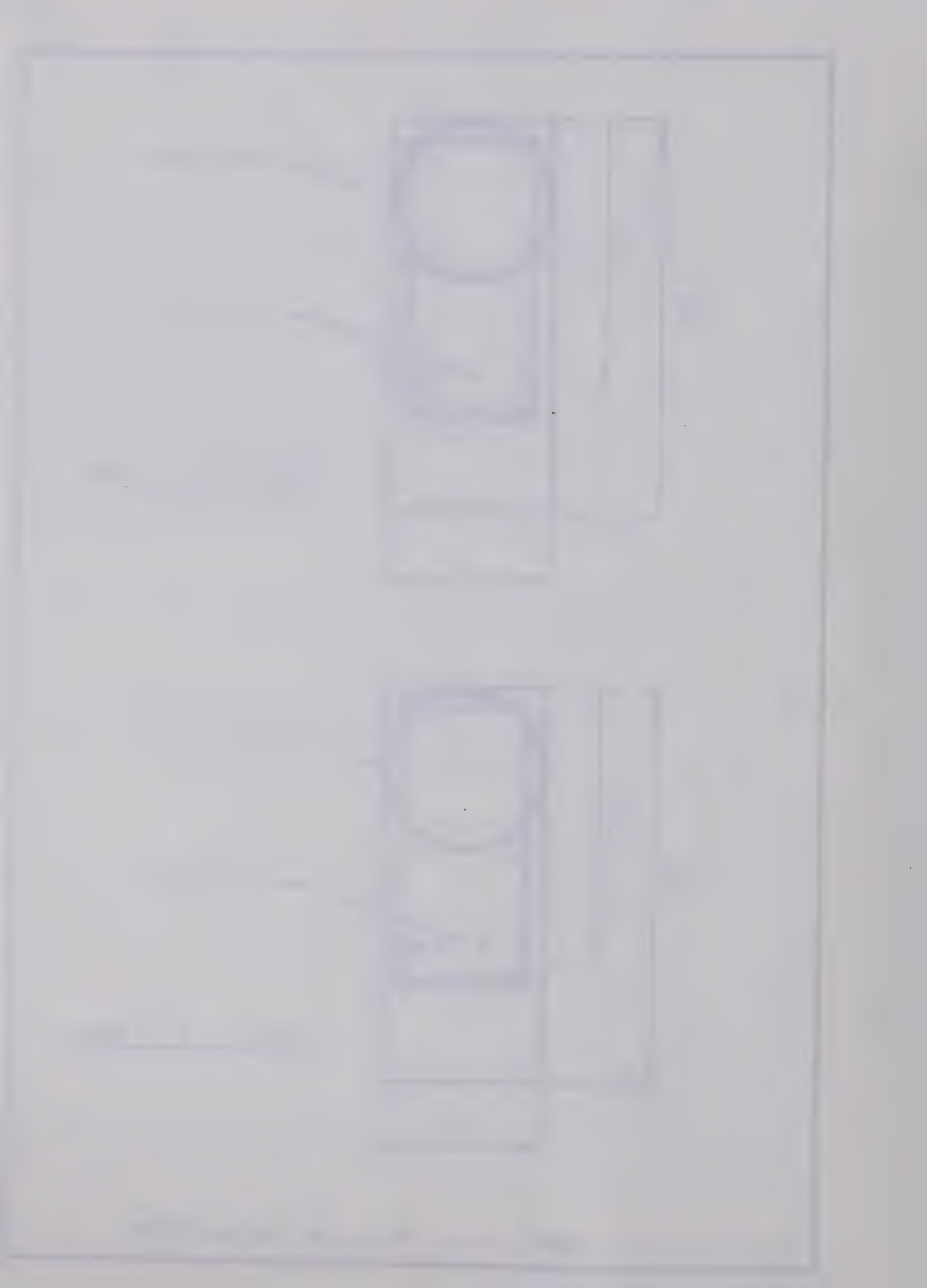

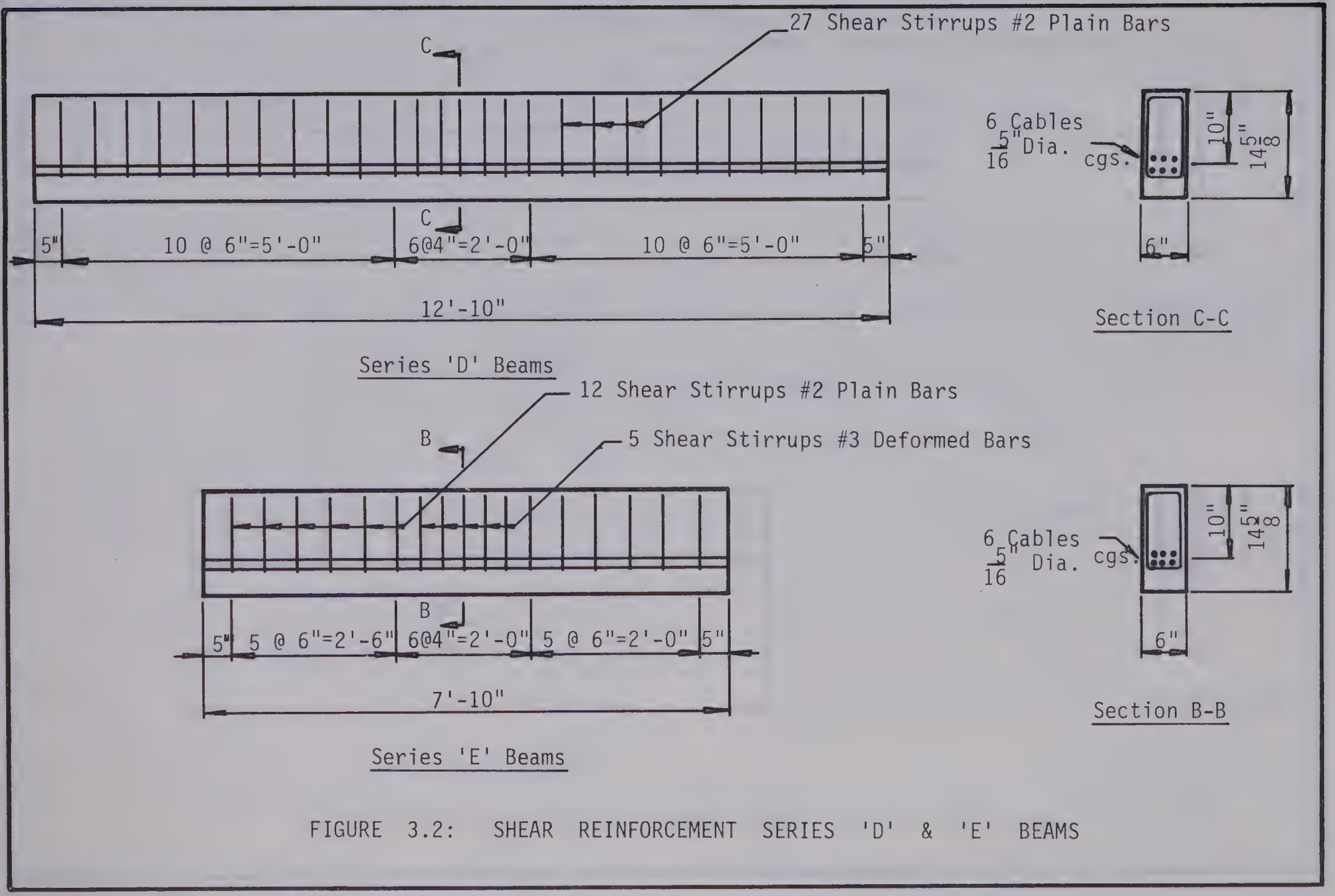

FIGURE 3.2: SHEAR REINFORCEMENT SERIES 'D' & 'E' BEAMS

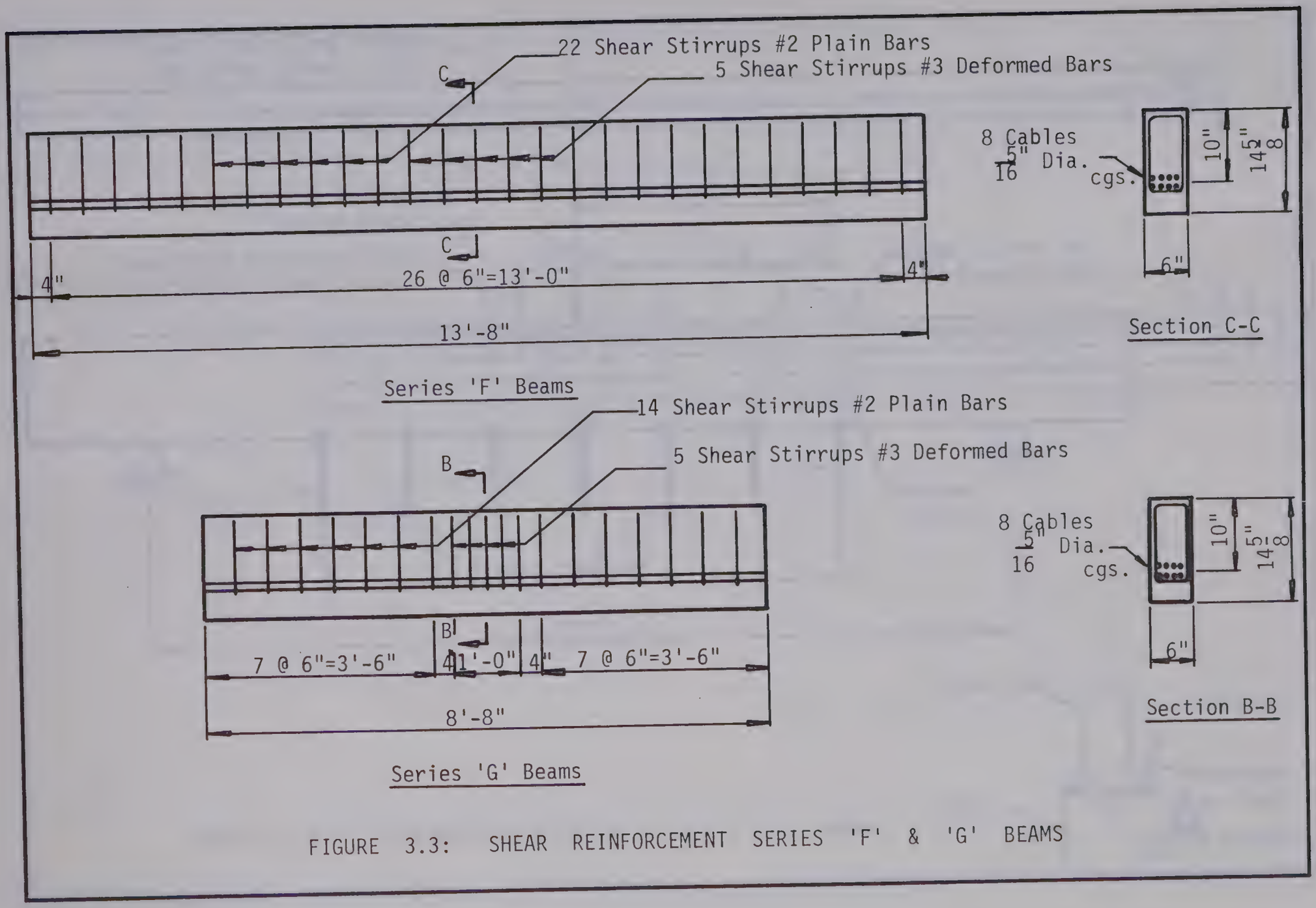

FIGURE 3.3: SHEAR REINFORCEMENT SERIES 'F' & 'G' BEAMS

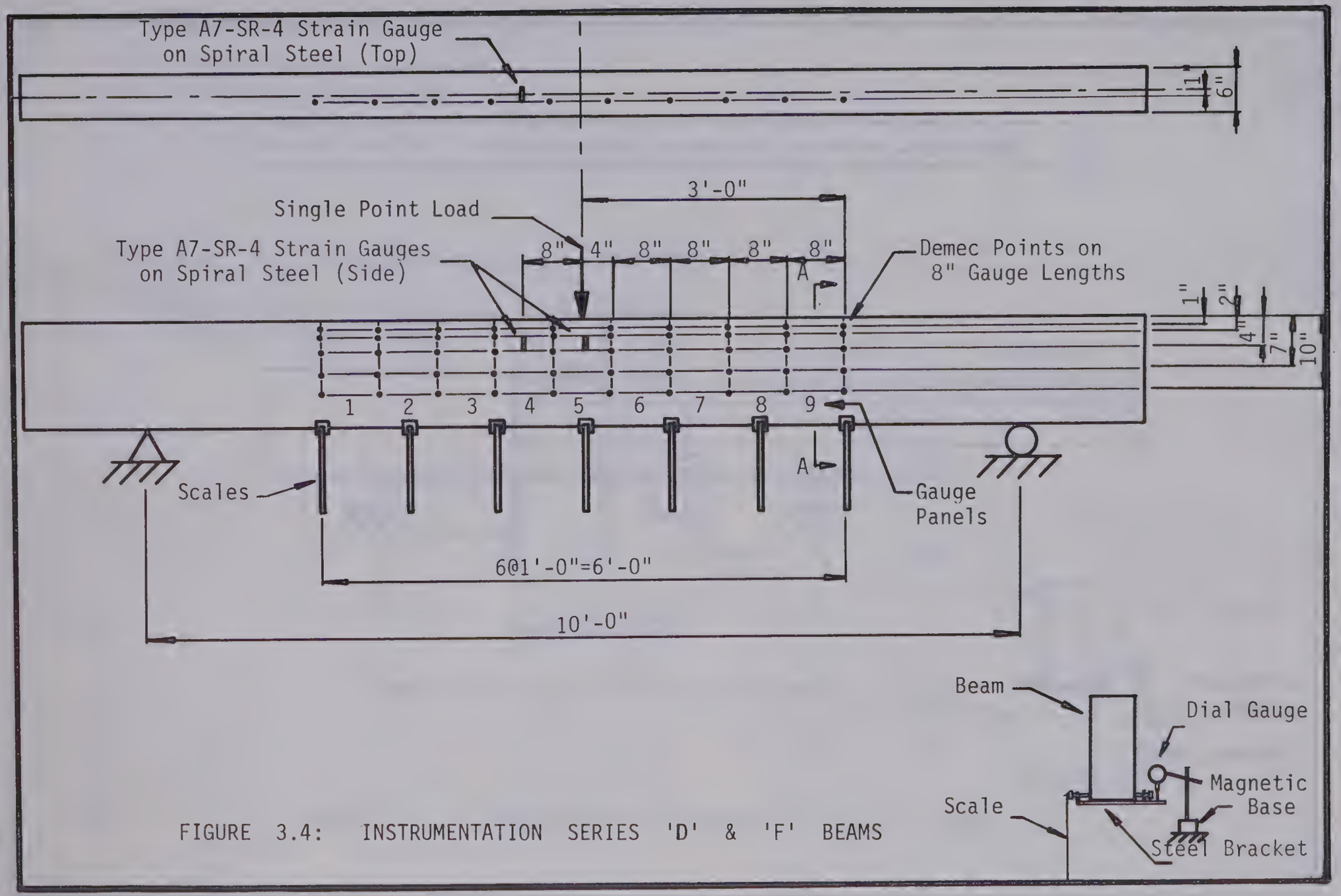

FIGURE 3.4: INSTRUMENTATION SERIES 'D' & 'F' BEAMS

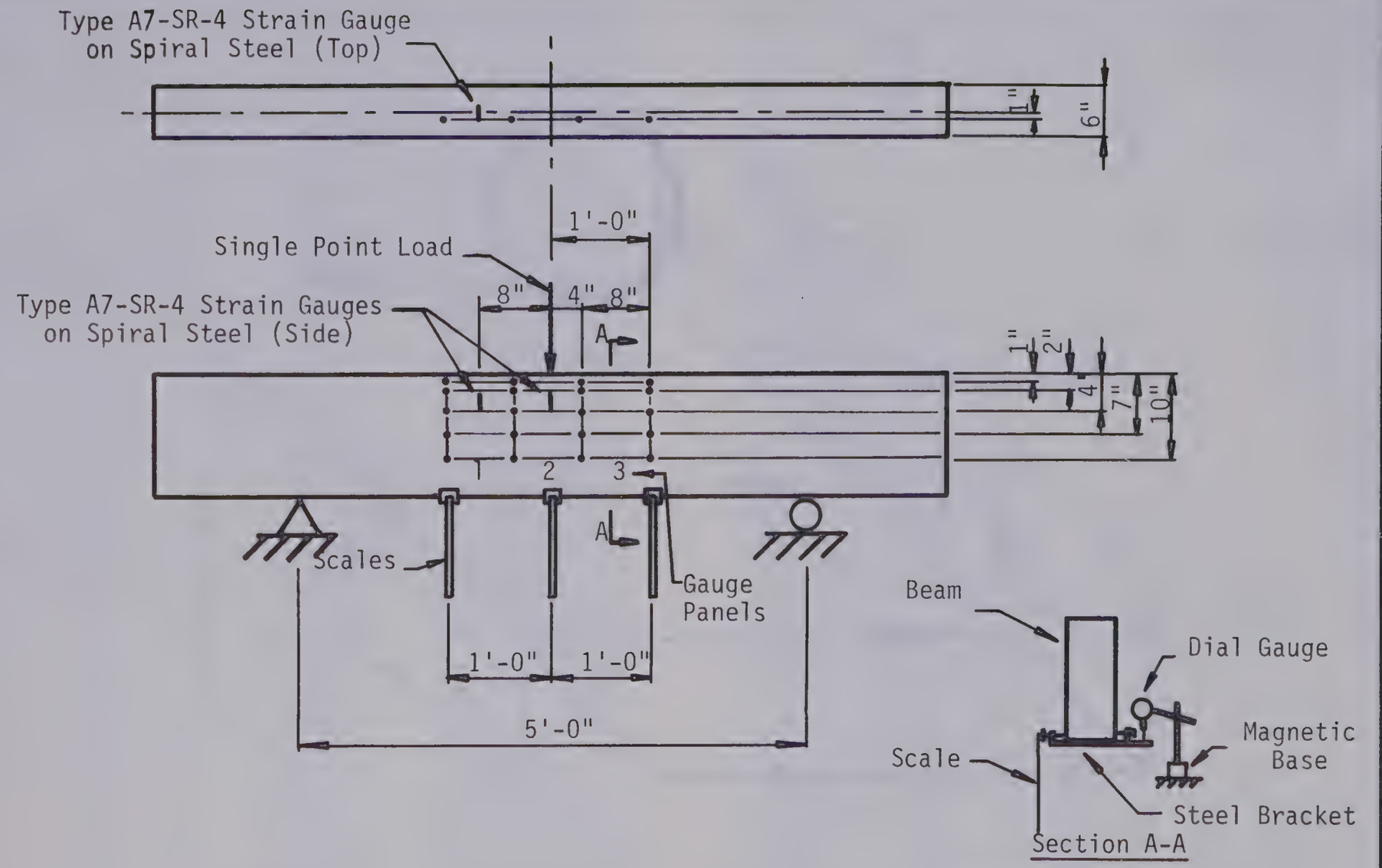

FIGURE 3.5: INSTRUMENTATION. SERIES 'E' & 'G' BEAMS

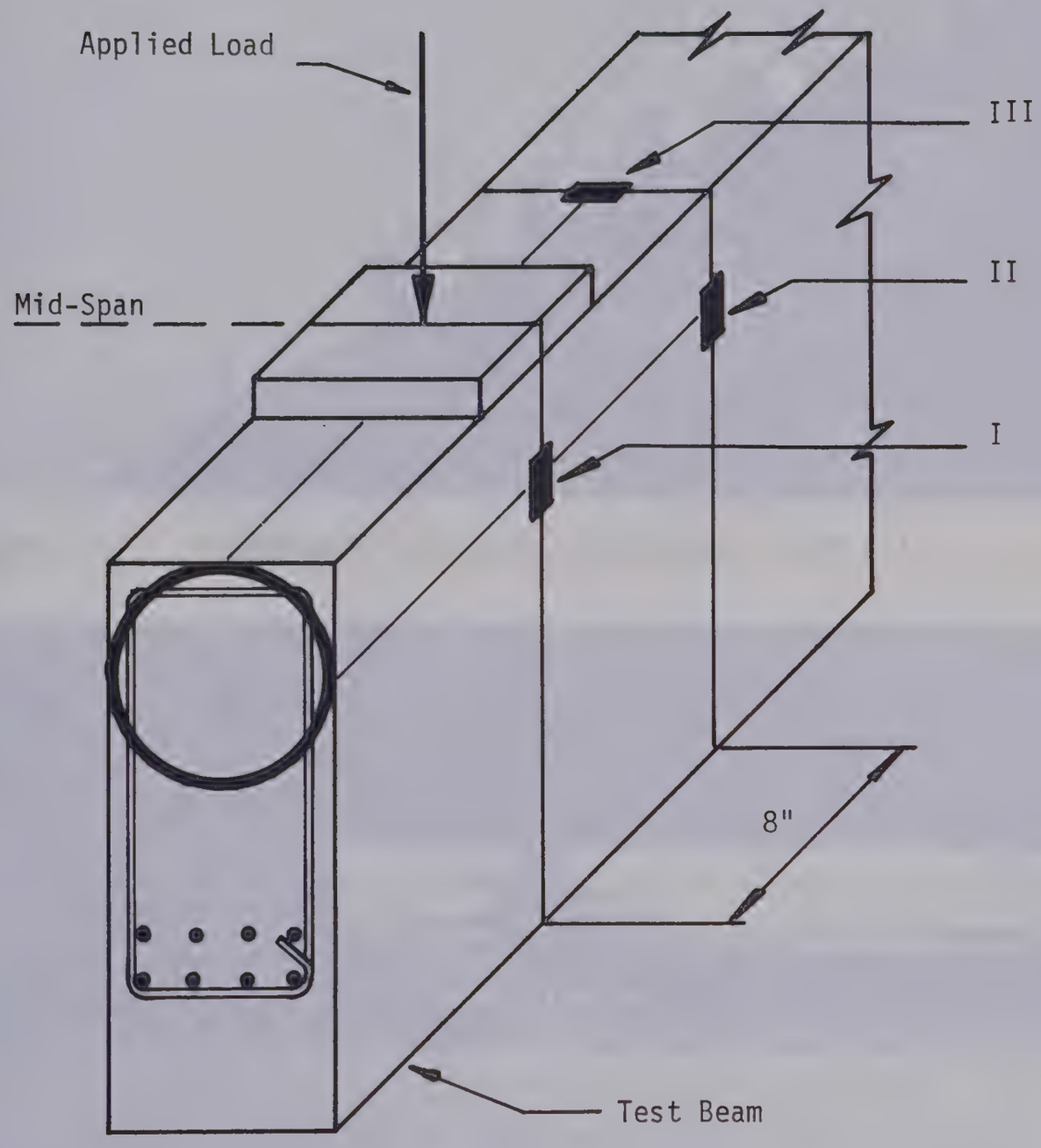

FIGURE 3.6: STRAIN GAUGES ON THE SPIRAL REINFORCEMENT

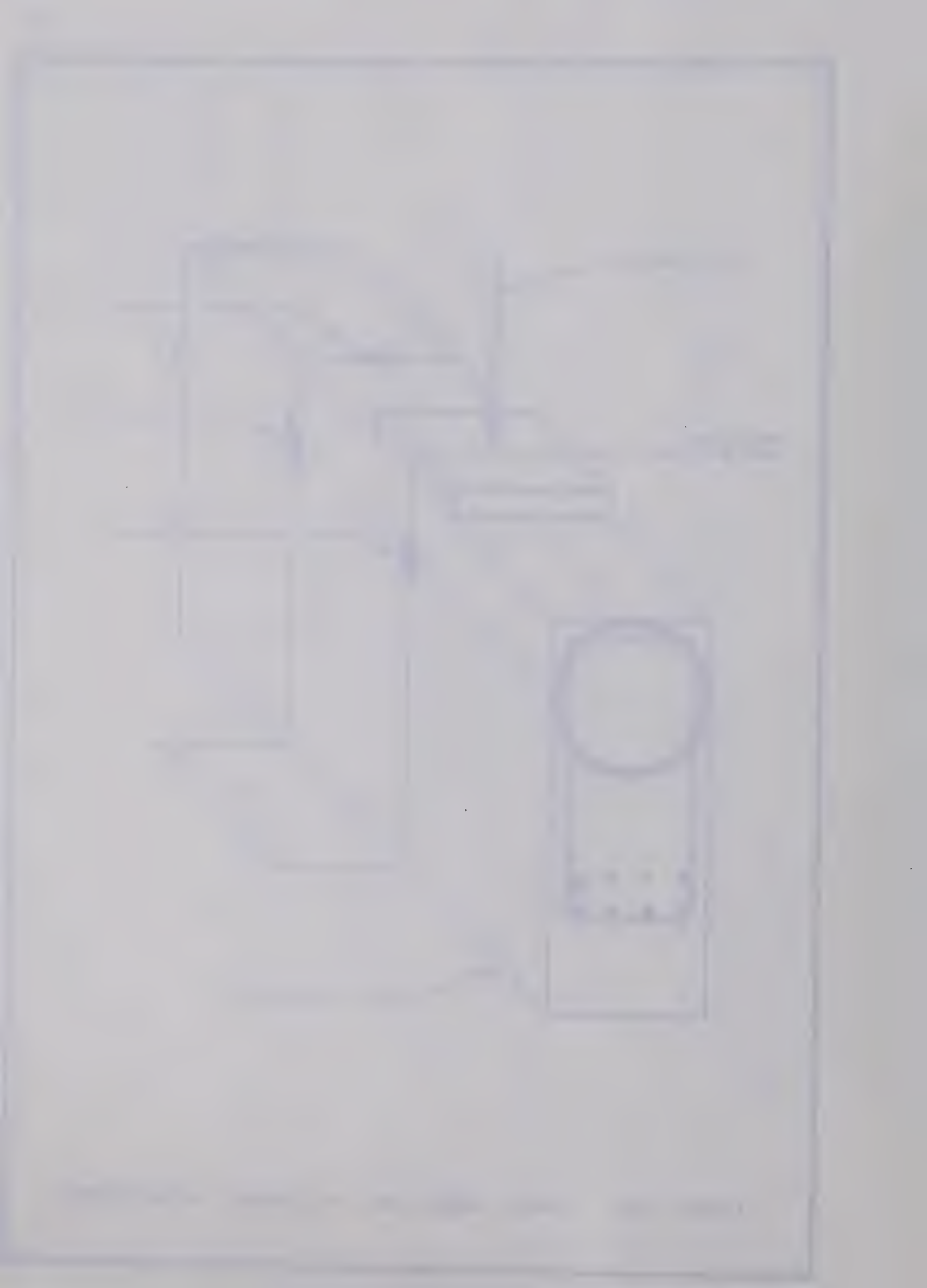

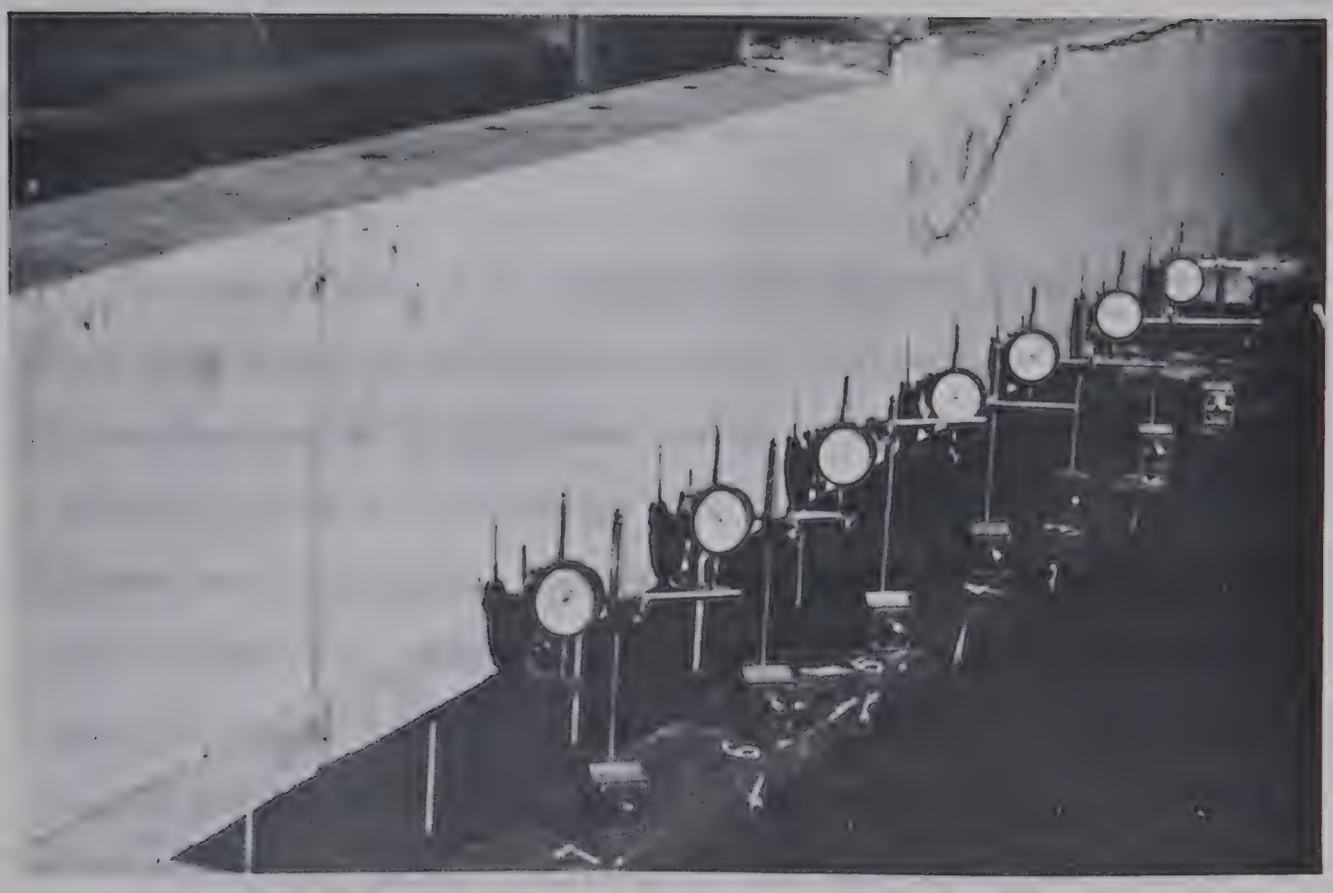

FIGURE 3.7: ARRANGEMENT OF DIAL GAUGES FOR BEAM F1

FIGURE 3.8: BEAM F1 PREPARED FOR TESTING

CHAPTER IV

TEST RESULTS

The test results of the beams are presented in terms of the measured load-deflection relationships shown in Figures 4.5 and 4.6, and the average strains in the extreme concrete compression fibres shown in Figures 4.7 and 4.8. The average strains were determined from measured deformations in the 8-in. gauge lengths of the instrumented region of the test beams. The derived moment-curvature relationships are presented in Figures 4.9 and 4.10, and Figures 4.11 to 4.14 show the variations in the spiral steel strains with respect to the applied moments. To illustrate the general behaviour of the test beams, the results for beam F1 are described in detail. Further details are presented in the discussion of test results in Chapter V.

The measured load-deflection relationship for beam F1 is presented in Figure 4.1. It shows four stages of behaviour. An initial linear portion, where the beam behaved elastically until first flexural cracking, was followed by a region where the rate of deflection increased for the applied load increments. This was terminated when crushing occurred at the top compression fibre. Beyond this, the rate of deflection increased further and a maximum load was reached just before the concrete spalled away and exposed the spiral reinforcement which confined the compression zone. A sudden reduction of load resistance is shown as a result of the reduced beam stiffness. In the final stage, the spiral reinforcement became effective in restraining the concrete

compression zone, and the load increased to nearly the maximum value reached at spalling before this beam finally failed in tension. The load reduction at spalling was not always observed in the other beams tested. After spalling, the beams resisted a level of load, at least equal to that reached at spalling, until fracture of the prestressed cables or rupture of the confined compression concrete occurred.

Figure 4.2 presents the moment-curvature relationship for beam F1. The curvatures were derived from the strains developed in the extreme compression fibre at mid-span, and the corresponding depths to the neutral axis determined from the average strain distributions for each load increment. The curvature was calculated using:

$$\psi = \frac{\varepsilon_c}{kd} \qquad (1)$$

After initial crushing, the curvatures were approximated from deflections measured using the precise level. The moment is presented in the non-dimensional form of M/M_i where M_i is the moment at the observed initial crushing of the extreme concrete compression fibre.

The average strain distributions over the effective depth of beam F1 for each 8-in. gauge panel length are presented in Figure 4.3. After the initial flexural cracking of beam F1, the strain distributions were determined by extending straight lines through the points representing the measured strains in the compression zone. Extensive cracking in the tension region made measured deformations in this region uncertain since they included the effect of crack openings. At initial crushing it is observed that the maximum concrete strain at the top compression

fibre occurs in panel four just to the left of mid-span. The influence of the spiral, the higher concrete strength, and the confining effect of the load bearing block may have rendered sufficient strength to the concrete causing the initial crushing to occur a short distance away from the bearing block. Similar plots were used to determine the strain distributions for the other beams.

Figure 4.4 shows the moment ratio M/M_i plotted against the strains in the spiral reinforcement at the gauge locations I, II and III shown in Figure 3.6. The yield strain of the spiral reinforcement was developed at location III when beam F1 reached its failure load. The magnitudes of the strains at locations I and II were considerably less.

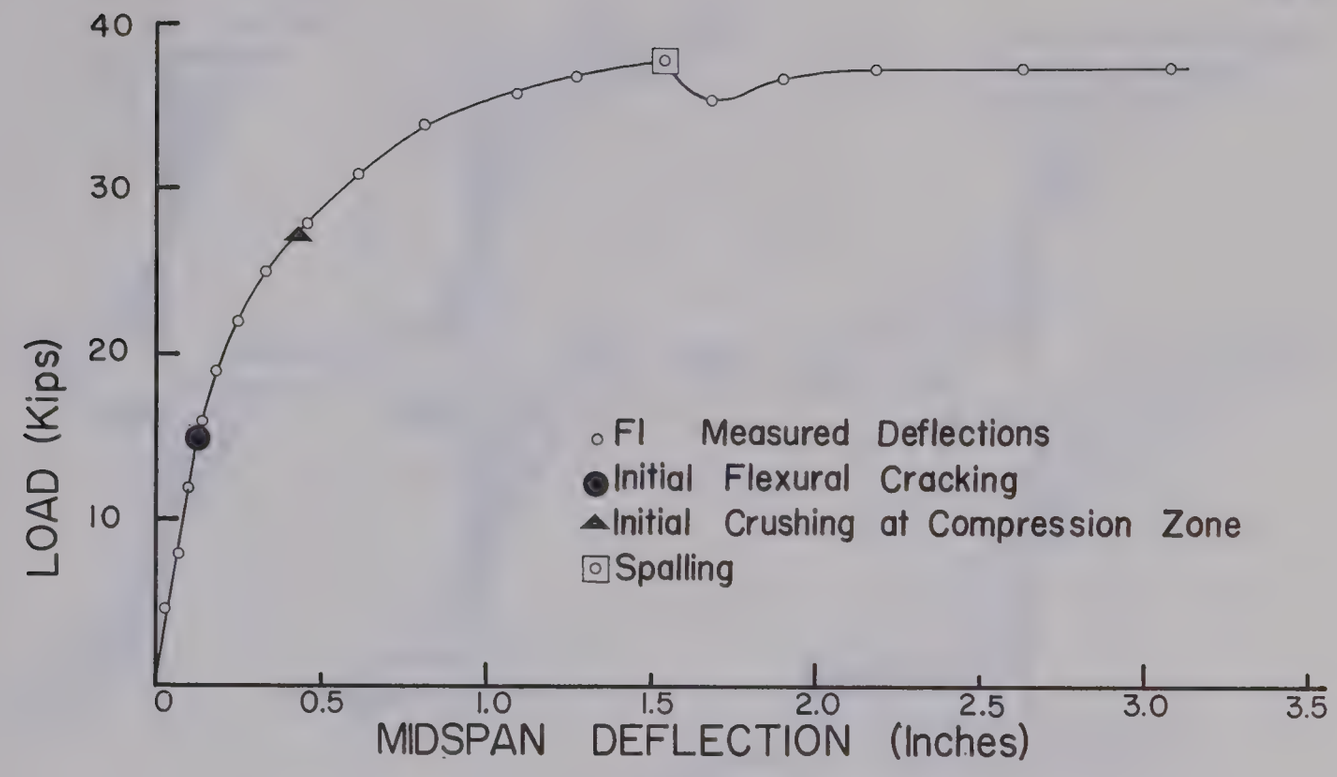

FIGURE 4.1

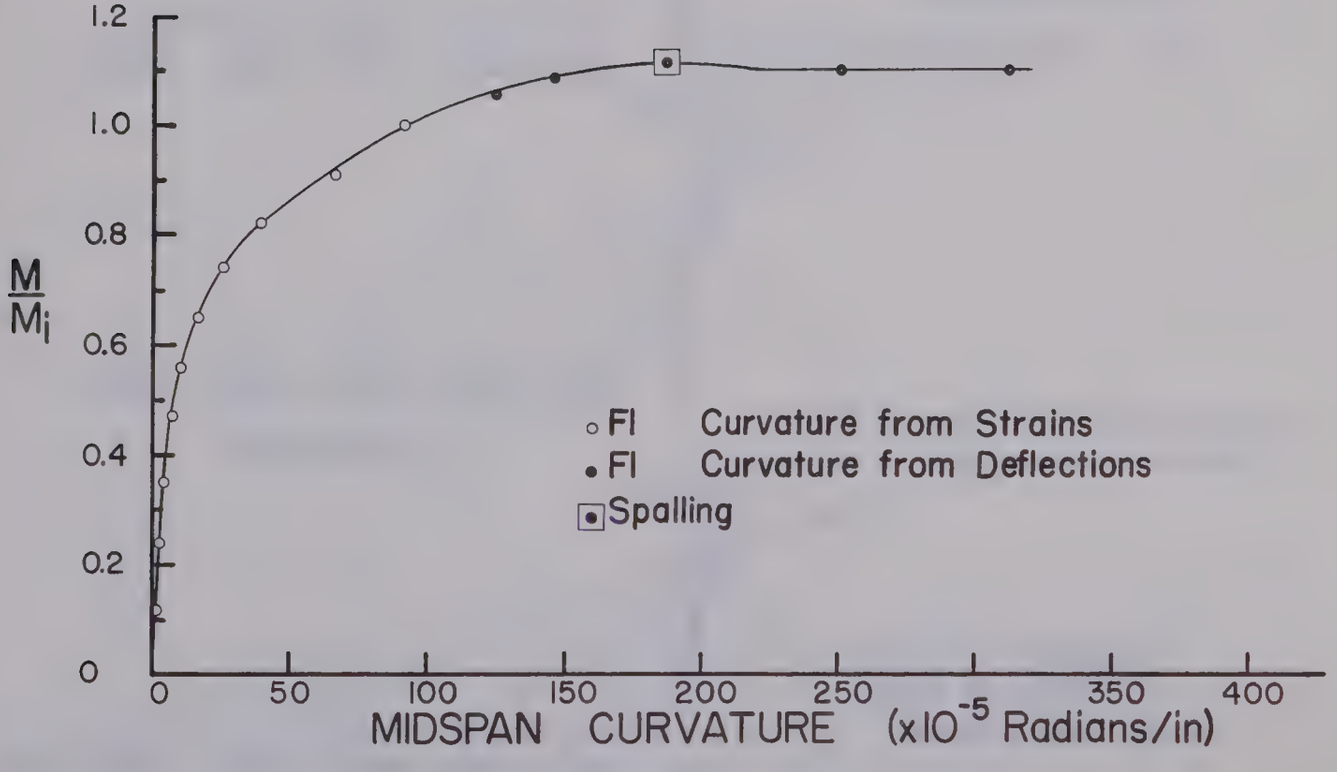

FIGURE 4.2

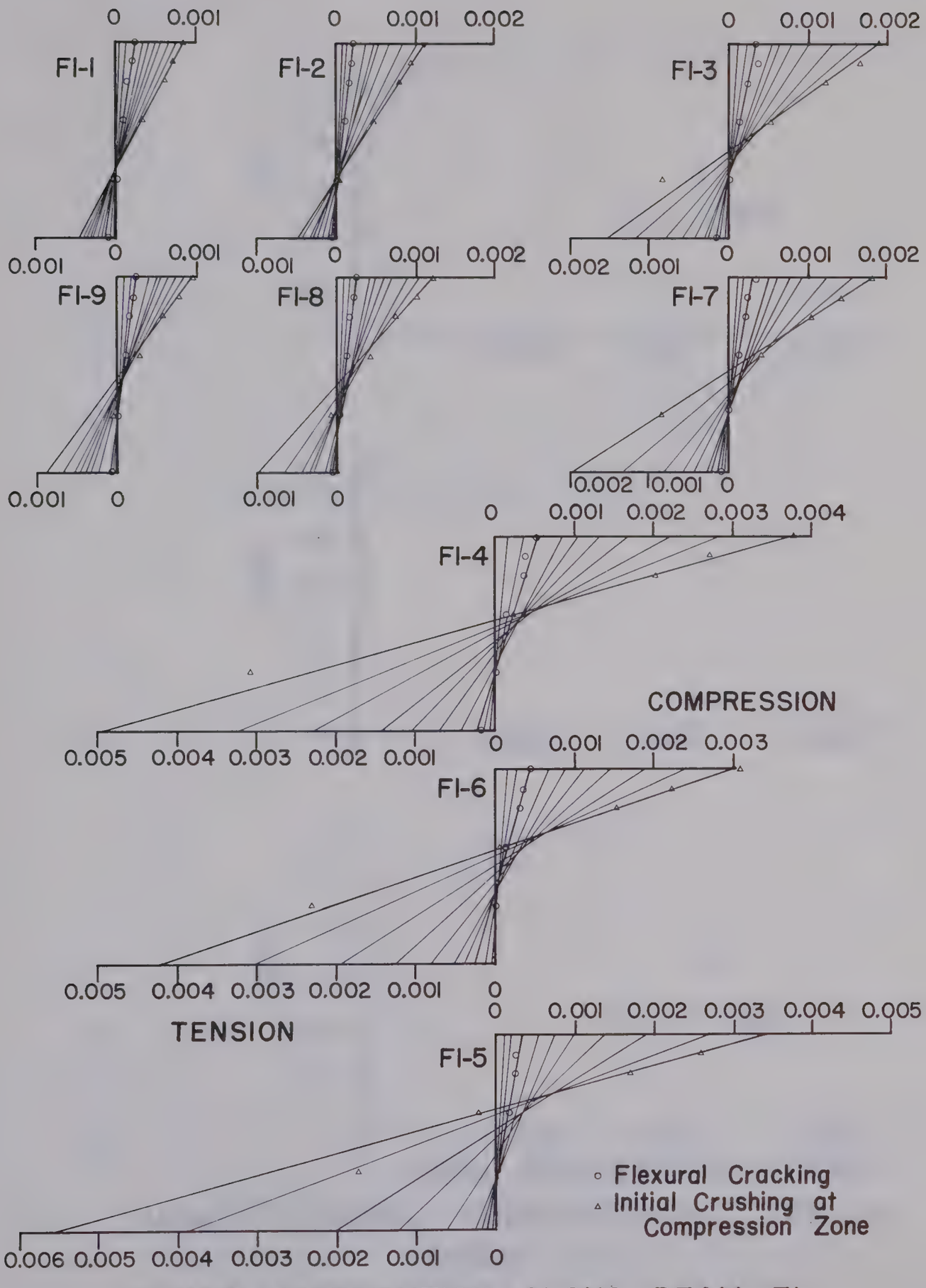

STRAIN DISTRIBUTION ALONG BEAM FI

FIGURE 4.3

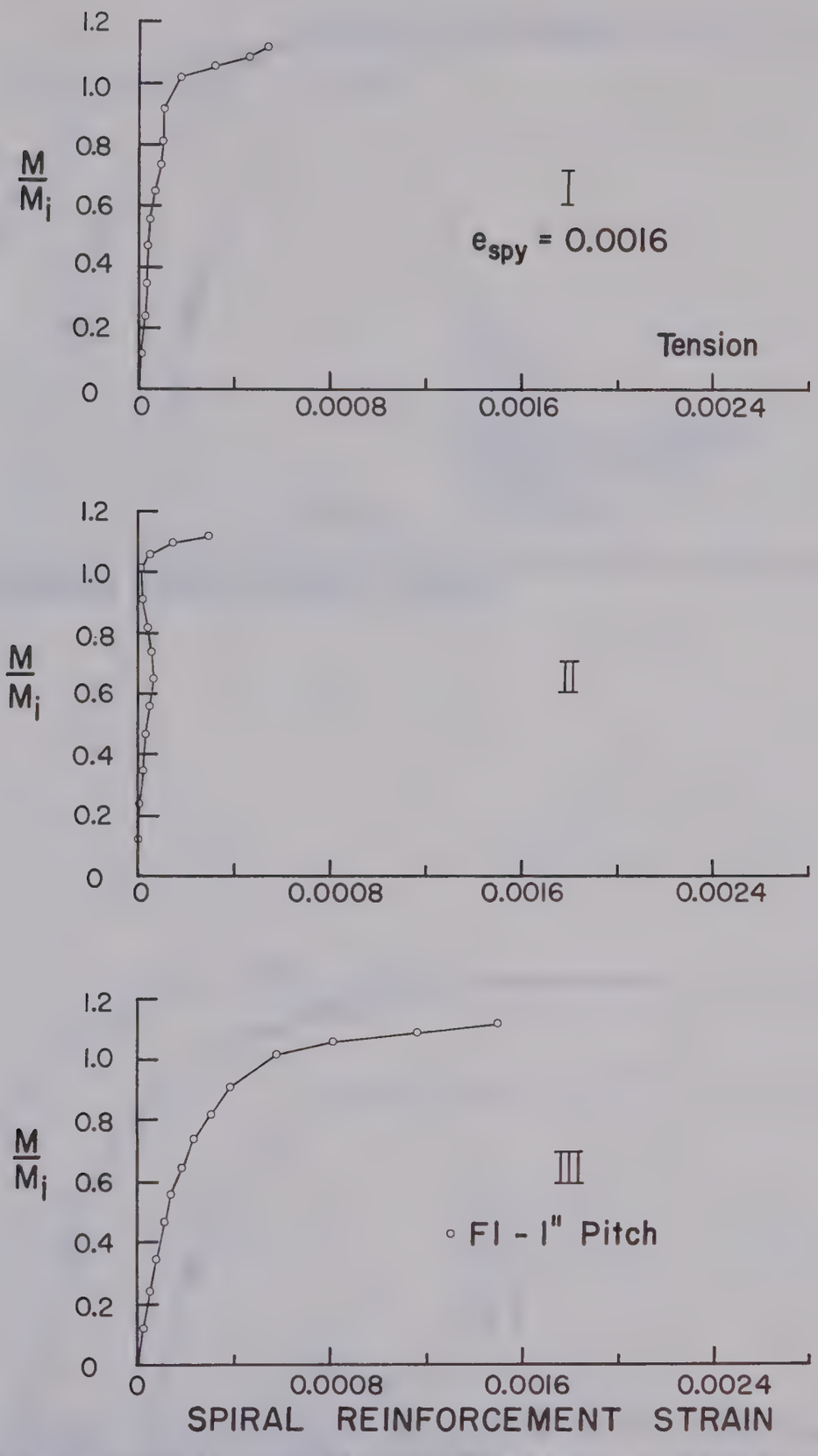

MOMENT v. SPIRAL REINFORCEMENT STRAIN
BEAM F1

FIGURE 4.4

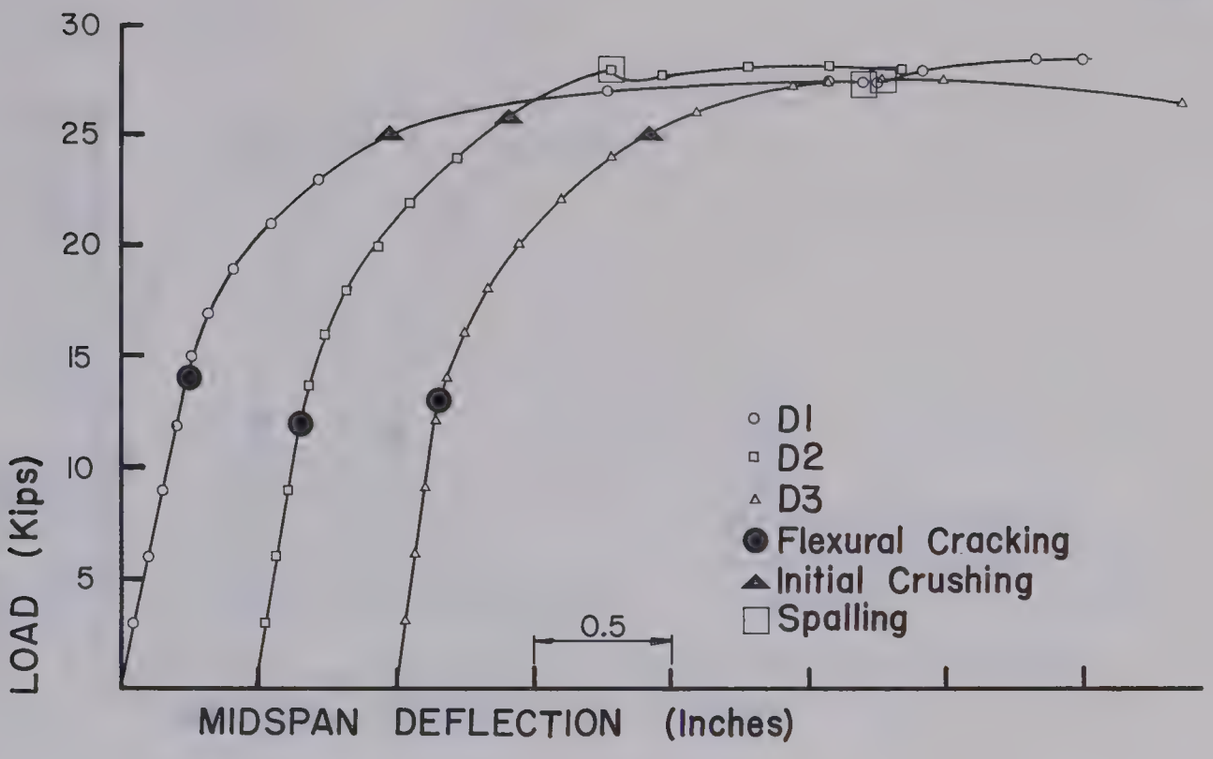

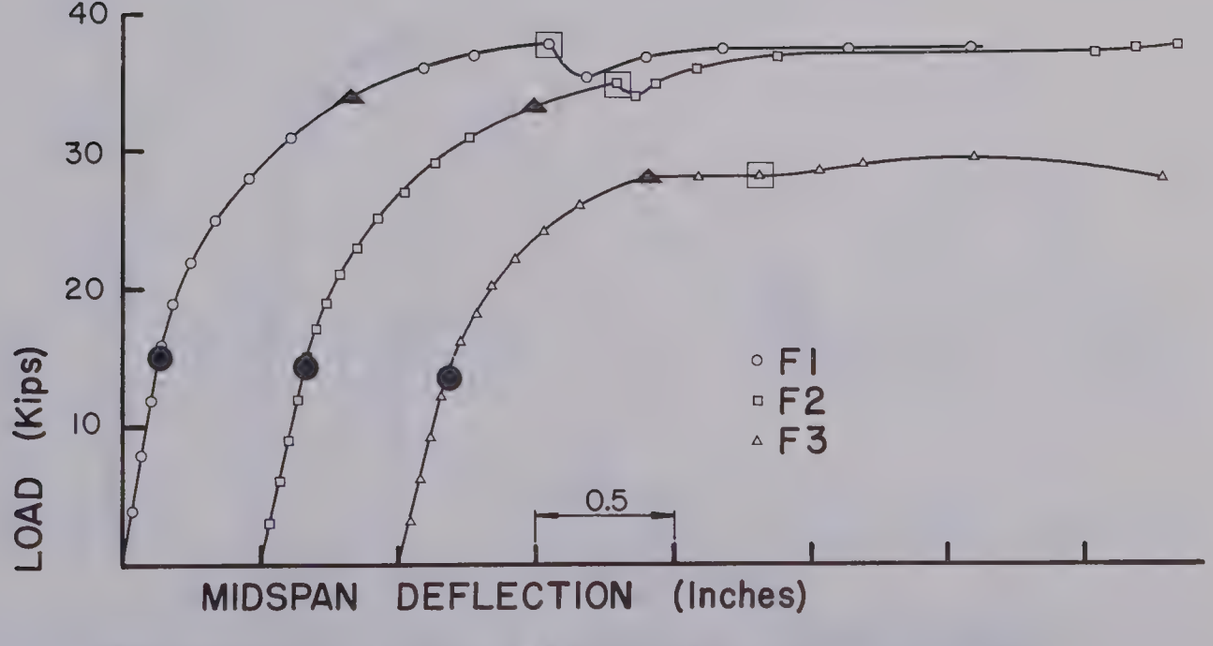

MEASURED LOAD v. MIDSPAN DEFLECTION DIAGRAMS SERIES 'D' & 'F' BEAMS

FIGURE 4.5

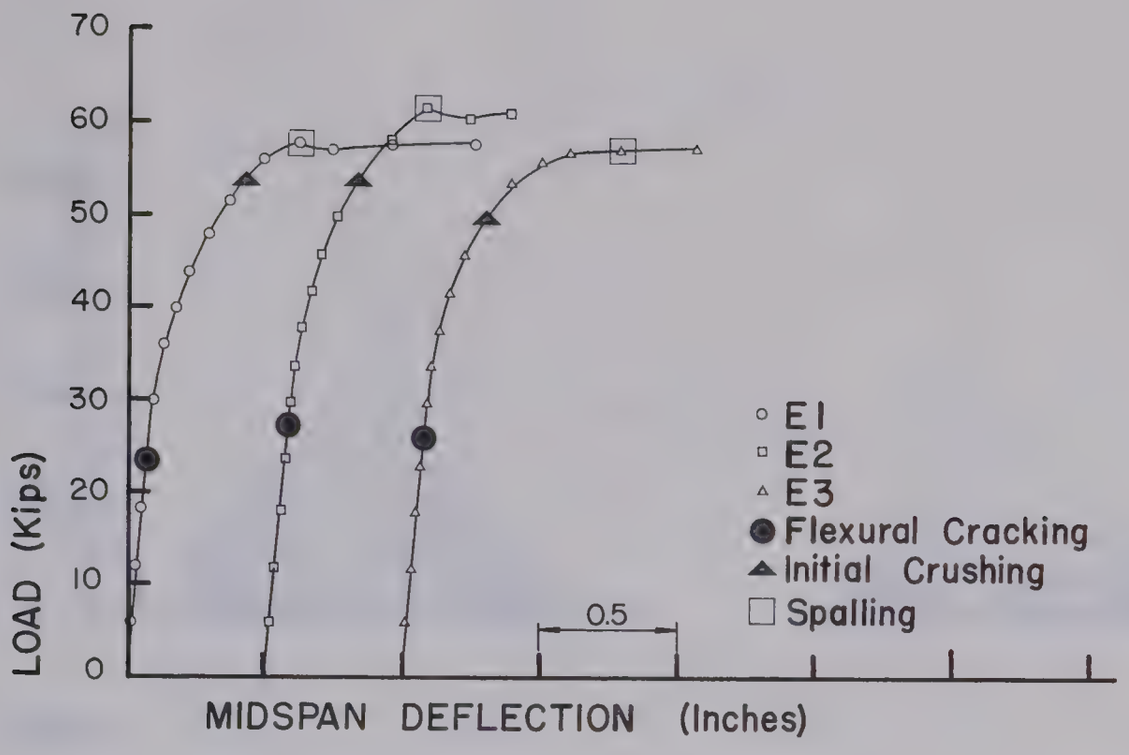

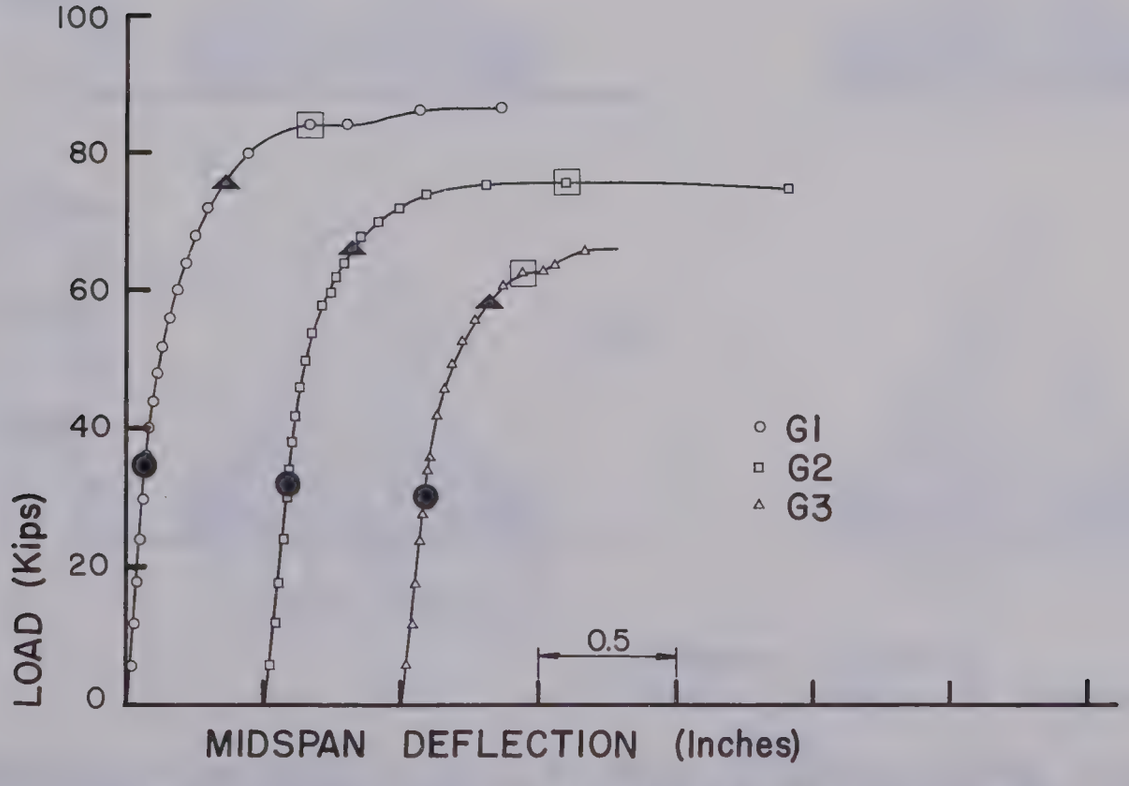

MEASURED LOAD v. MIDSPAN DEFLECTION DIAGRAMS SERIES 'E' & 'G' BEAMS

FIGURE 4.6

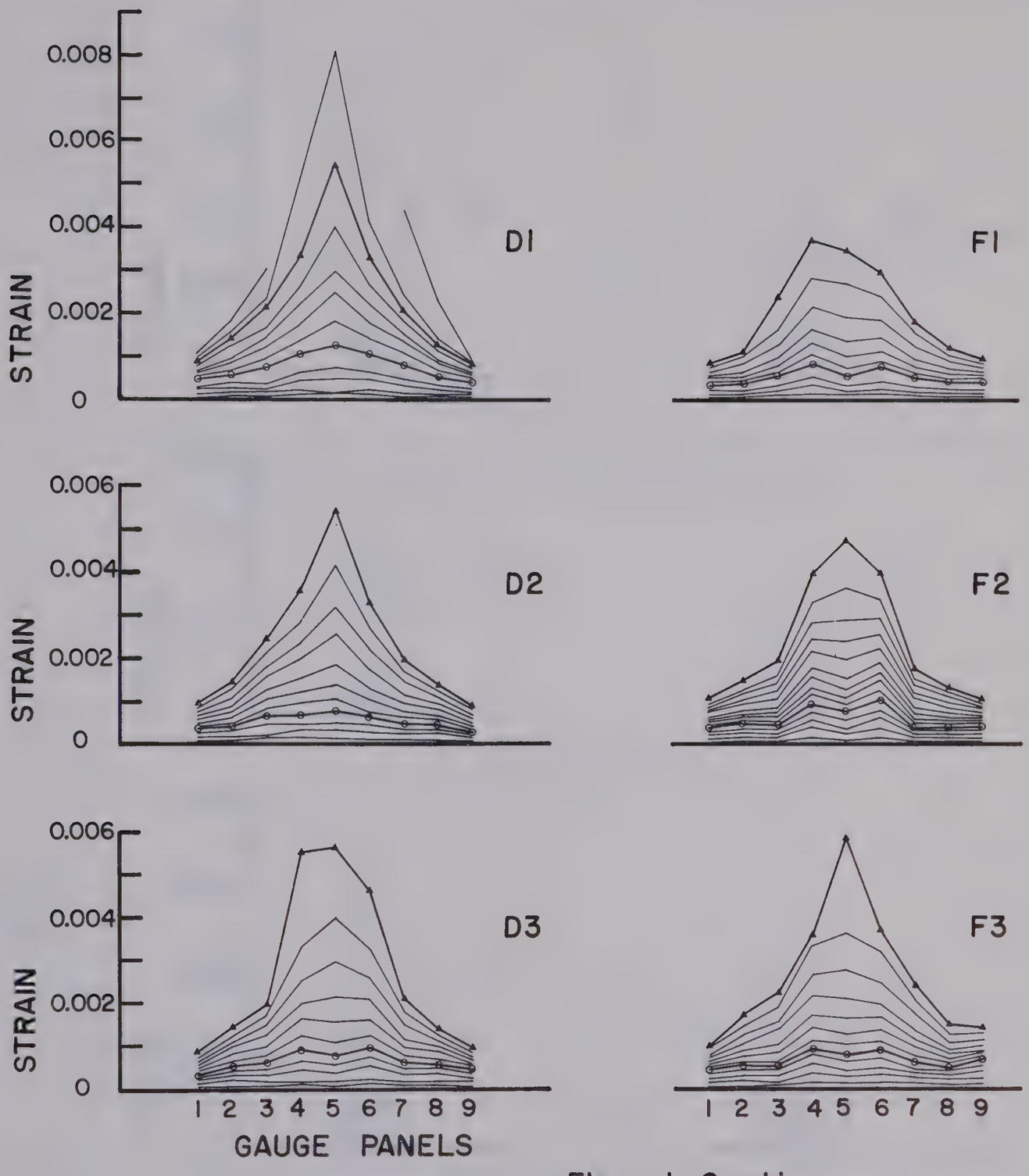

STRAIN DISTRIBUTION AT TOP COMPRESSION FIBRE FOR SERIES 'D' & 'F' BEAMS

FIGURE 4.7

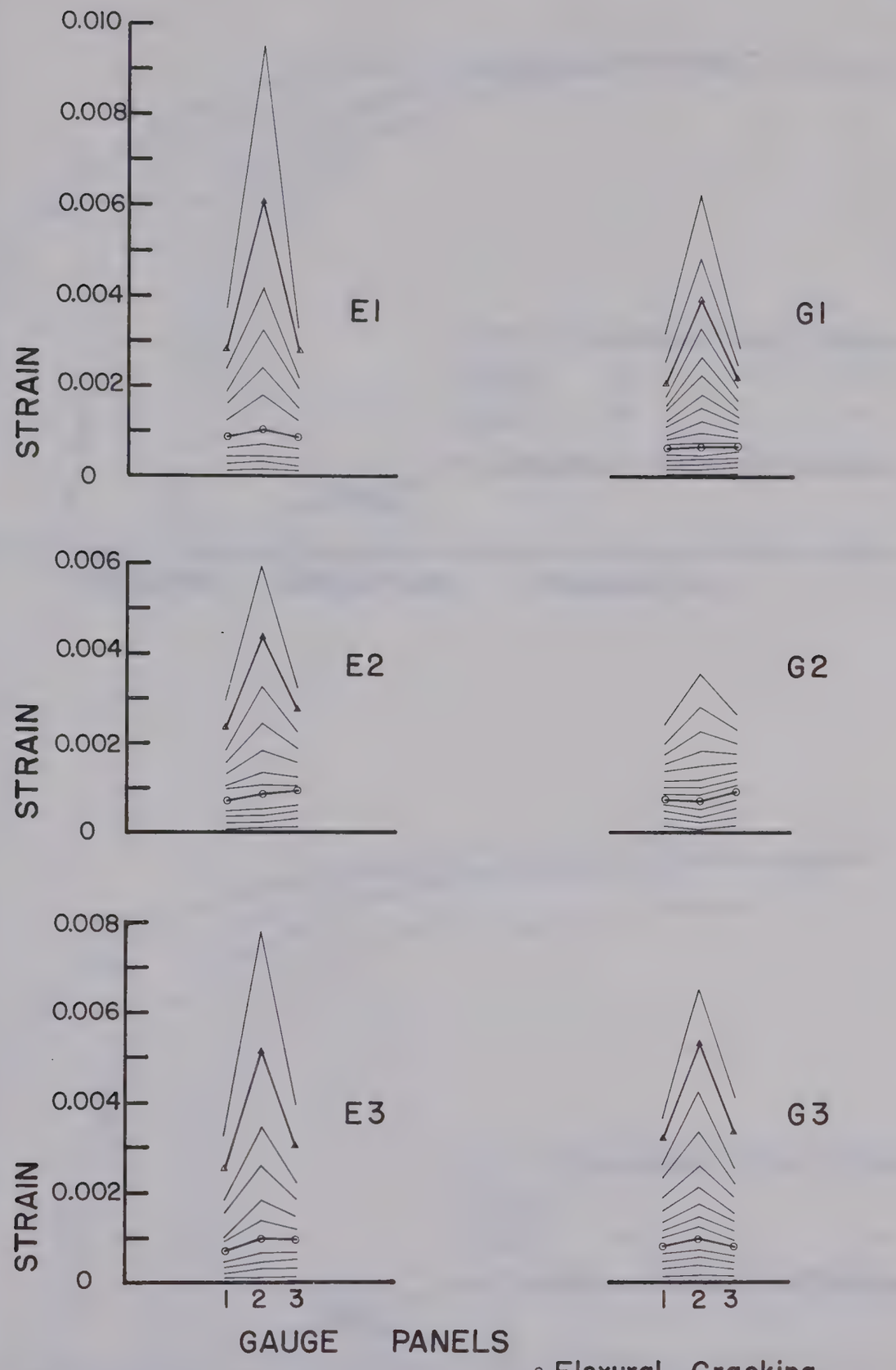

STRAIN DISTRIBUTION AT TOP COMPRESSION FIBRE FOR SERIES 'E' & 'G' BEAMS

FIGURE 4.8

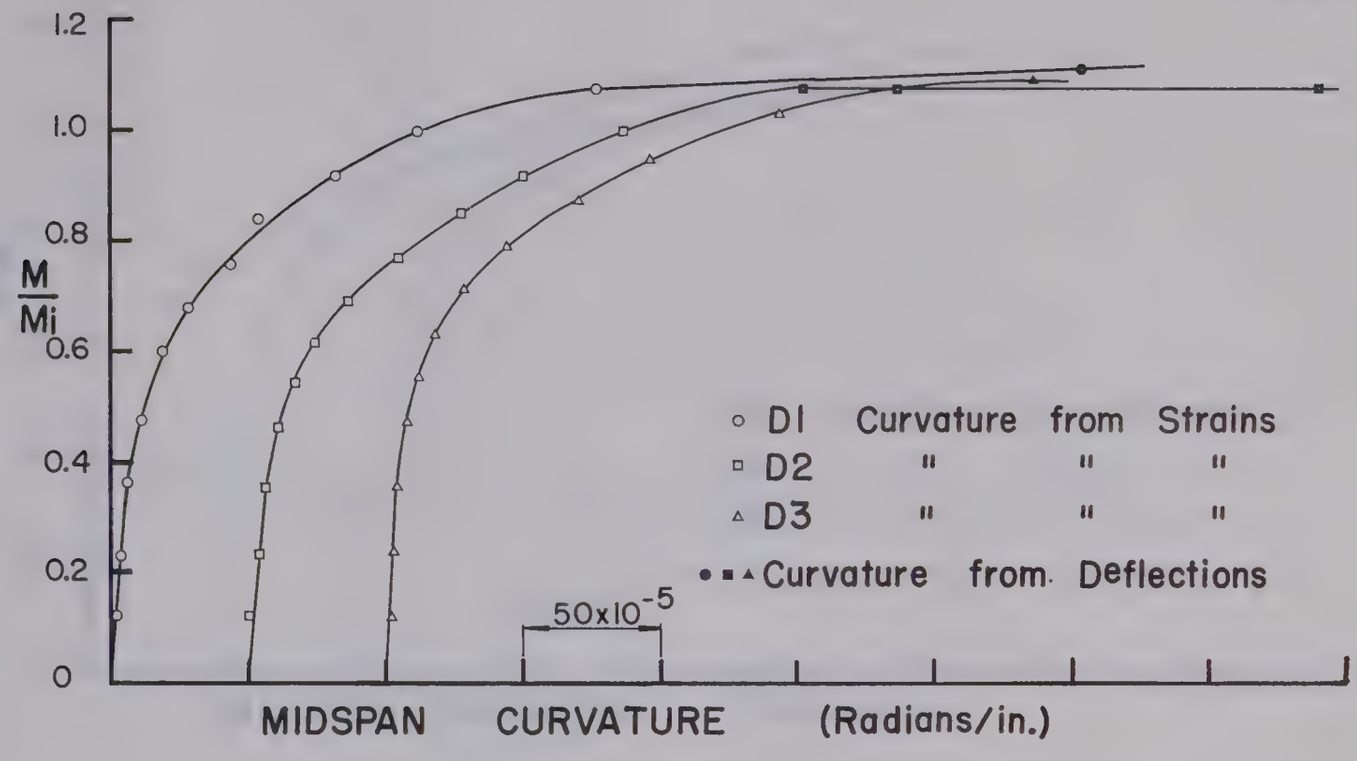

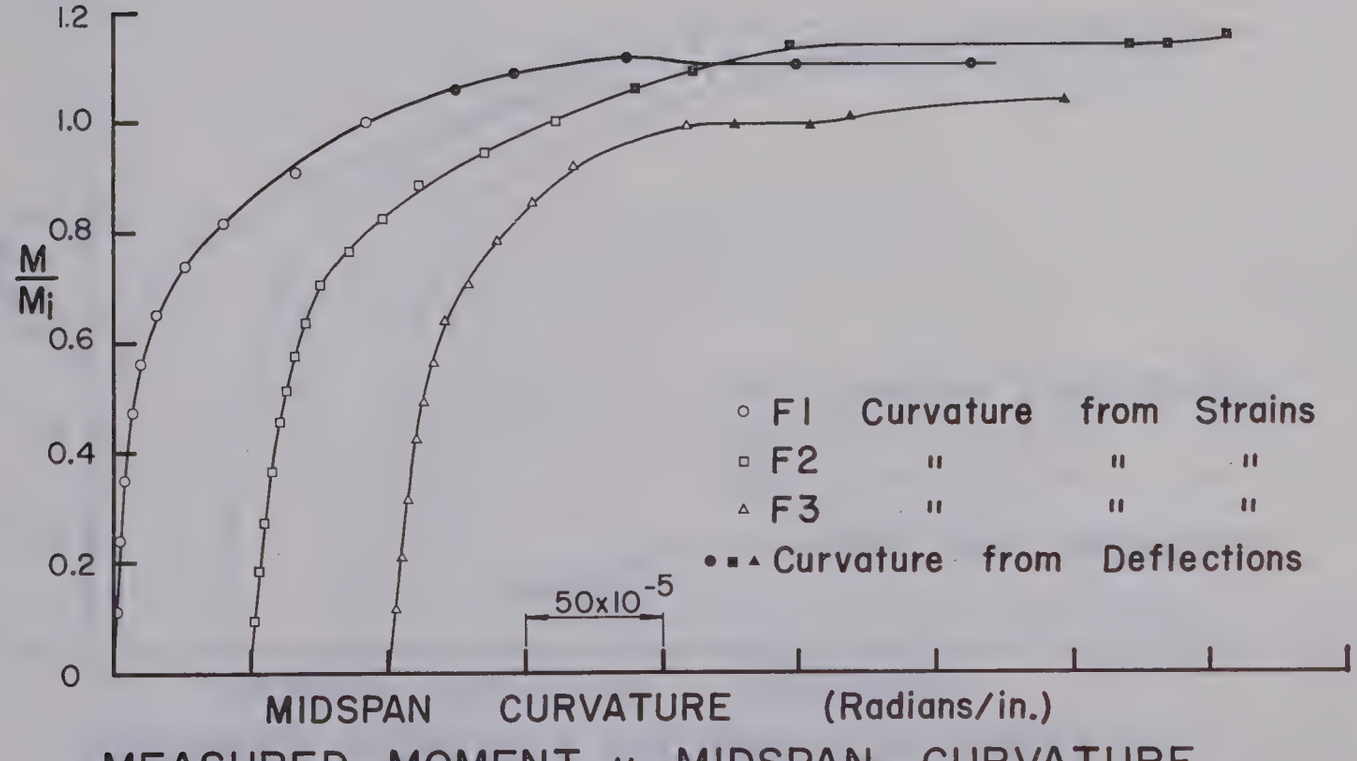

MEASURED MOMENT v. MIDSPAN CURVATURE DIAGRAMS SERIES 'D' & 'F' BEAMS

FIGURE 4.9

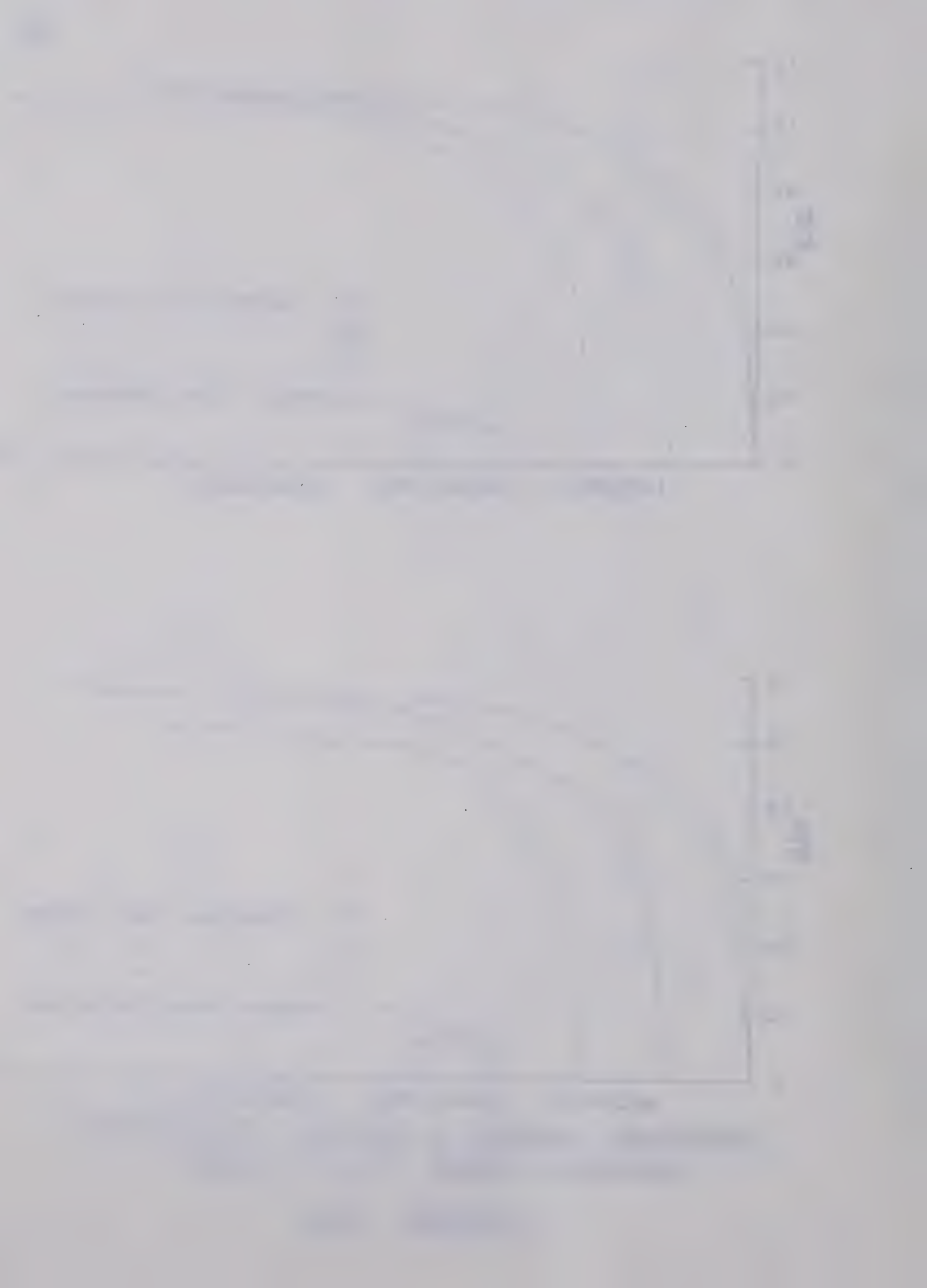

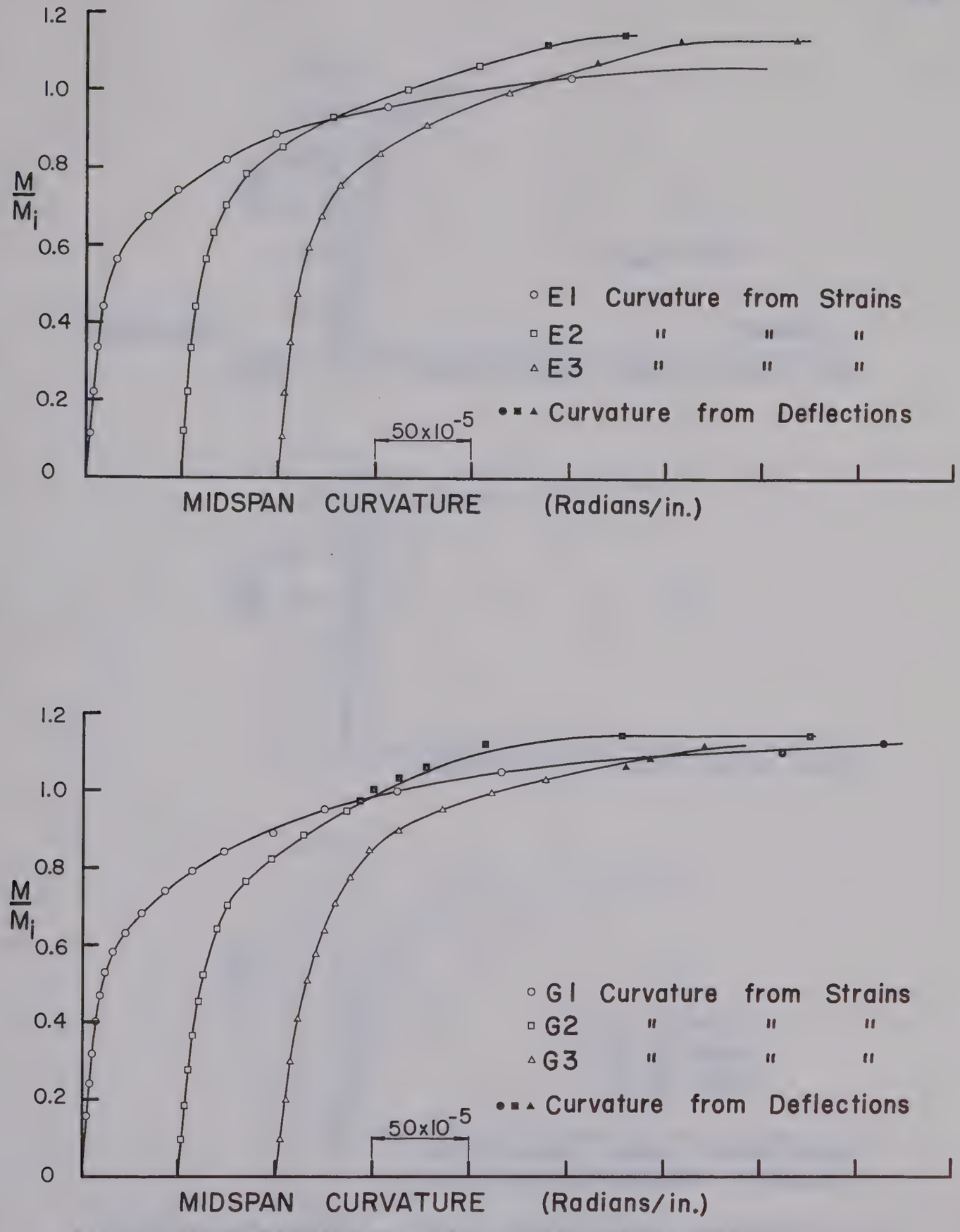

MEASURED MOMENT v. MIDSPAN CURVATURE DIAGRAMS SERIES 'E' & 'G' BEAMS

FIGURE 4.10

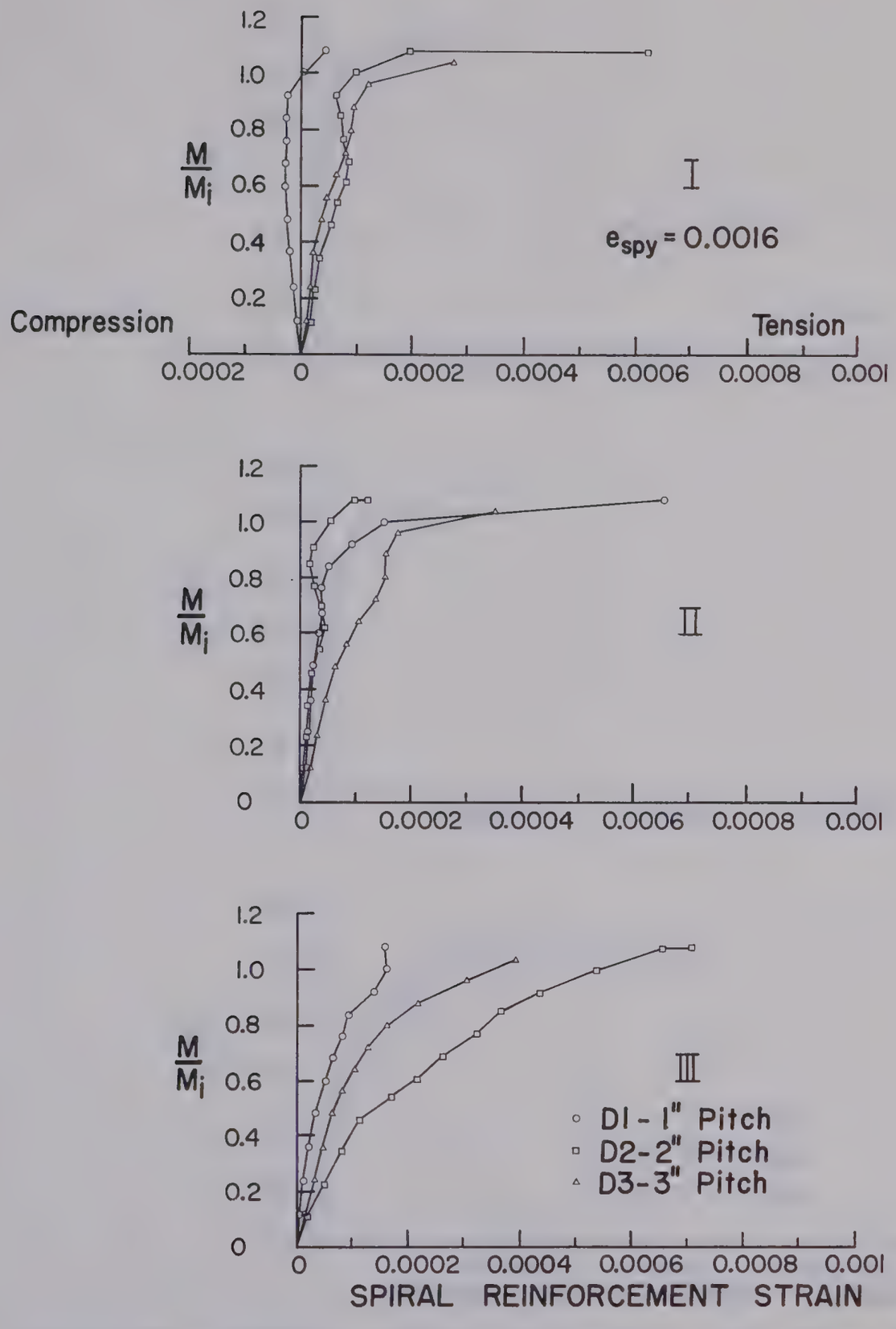

MOMENT v. SPIRAL REINFORCEMENT STRAIN
SERIES 'D' BEAMS

FIGURE 4.11

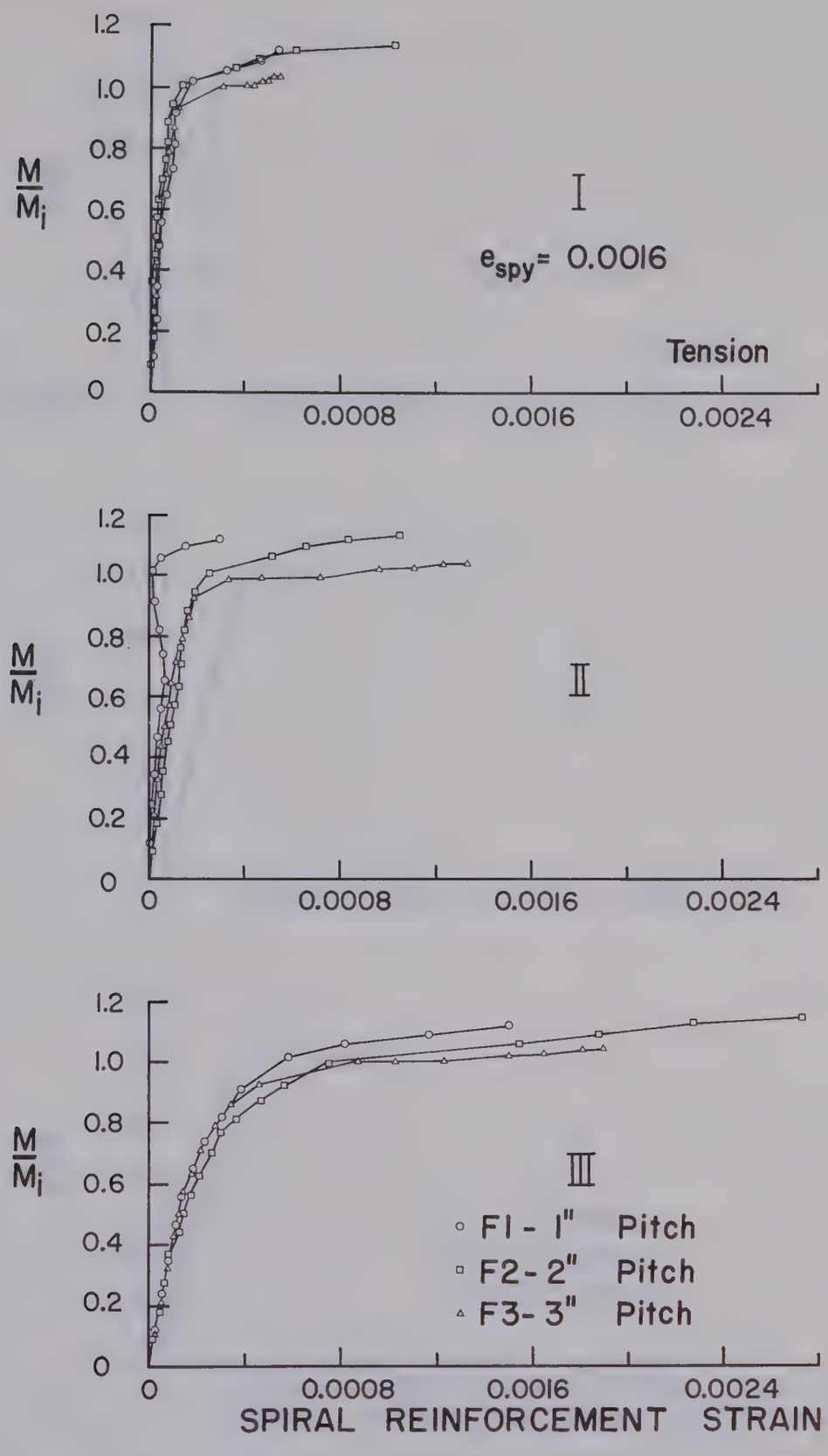

MOMENT v. SPIRAL REINFORCEMENT STRAIN
SERIES 'F' BEAMS

FIGURE 4.12

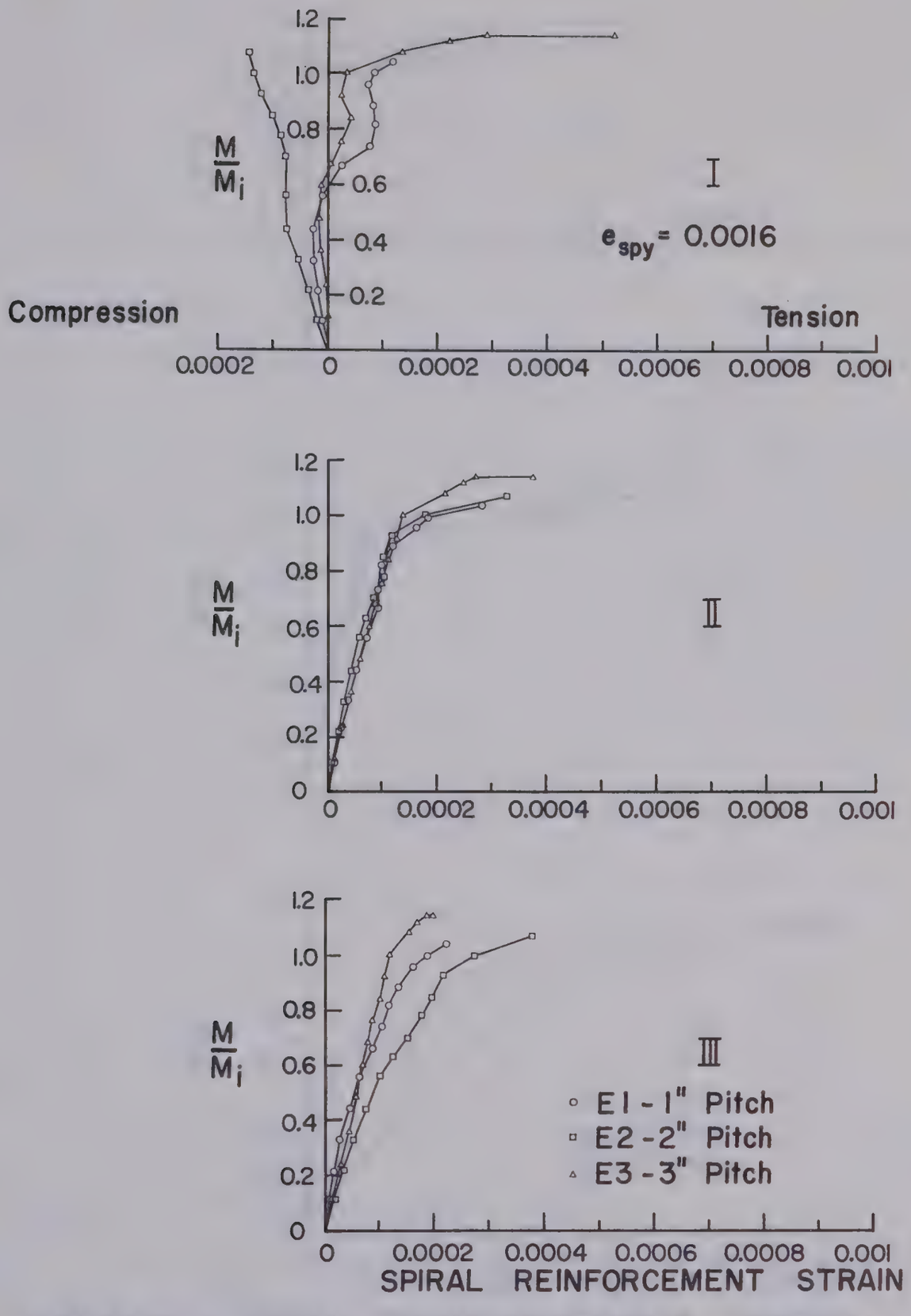

MOMENT v. SPIRAL REINFORCEMENT STRAIN
SERIES 'E' BEAMS

FIGURE 4.13

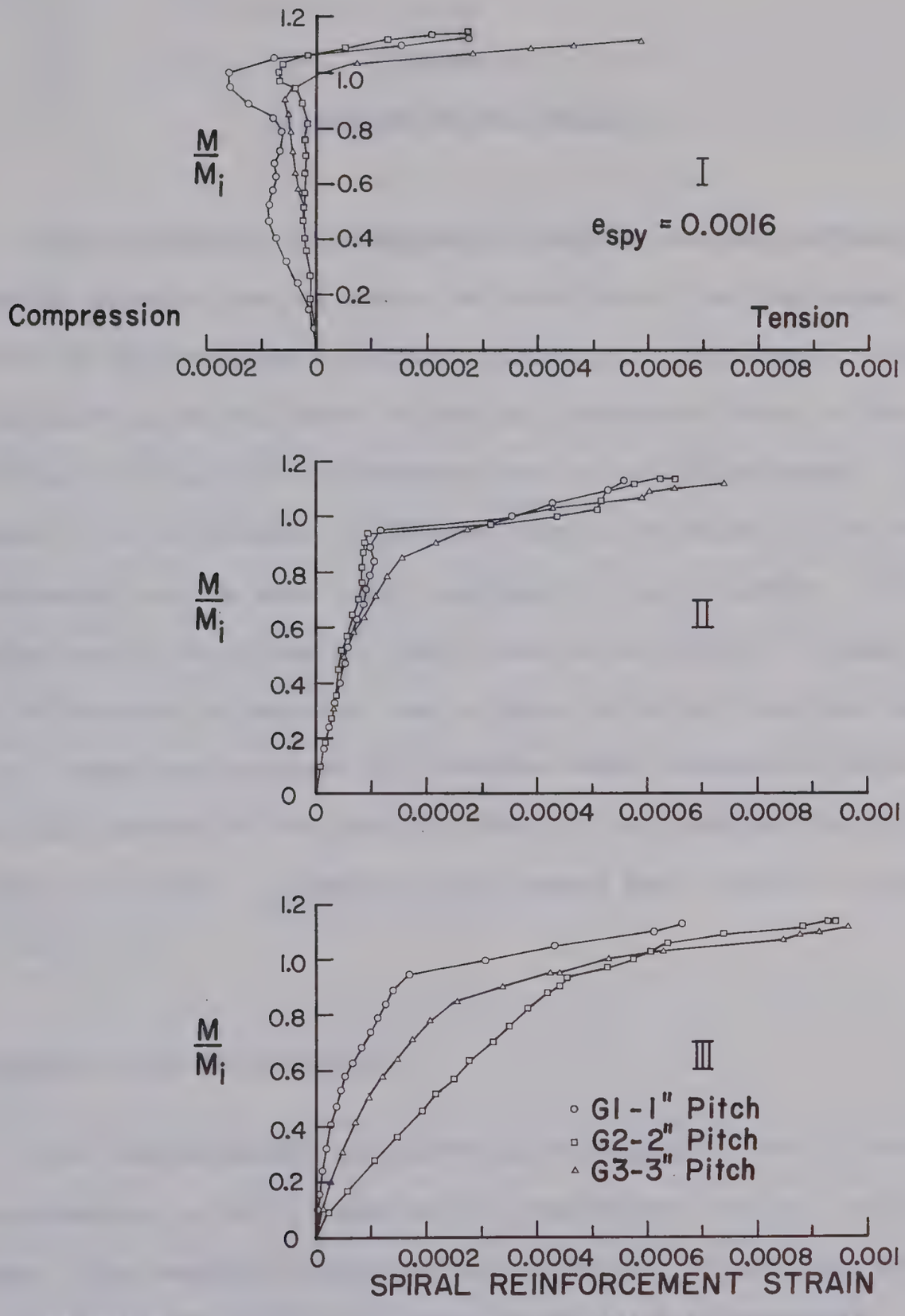

MOMENT v. SPIRAL REINFORCEMENT STRAIN

SERIES 'G' BEAMS

FIGURE 4.14

CHAPTER V

DISCUSSION OF TEST RESULTS

The test results are discussed in terms of how the confined compressed concrete zone influences the behaviour of the test beams. The effect of the confinement on the load-deflection and moment-curvature relationships, on the strain in the top compression fibre, on the strains in the spiral reinforcement, and on the failure modes is discussed. The differences in behaviour due to the amount of tension reinforcement and the span length are noted in the discussion. Although variations in the concrete strength were not originally intended, apparent differences in behaviour due to these variations have been noted. Brief comparisons are made with previous tests conducted by Belke (3), and some comments on the over-all effect of the confined compression zone are included. A summary of the present test results is presented in Table 5.2.

LOAD-DEFLECTION RELATIONSHIPS

The load-deflection relationships in Figures 4.5 and 4.6 show that the behaviour to initial compression crushing was similar for all the beams. The behaviour beyond initial compression crushing depended on the degree of confinement provided by the spiral reinforcement. Figure 4.5 shows that beams D1 and F1 deflected more between initial crushing and spalling than the other beams in their series. After spalling,

three types of behaviour were observed:-

(1) a sudden reduction of load resistance in beams D2, F1 and F2. The load resistance just prior to spalling was restored after a redistribution of stresses;

(2) a continuously increasing load resistance in beams D1 and F3;

(3) a reduced load resistance in beam D3.

Figure 4.6 shows similar types of behaviour in series E and G beams.

Higher concrete strengths and amounts of tension reinforcement generally showed greater load capacities, and in some cases, increased deflections. The load capacities of the short span beams were at least twice those resisted by the long span beams. The deflections varied between 30% and 60% of the values obtained for the corresponding long span beams.

STRAIN VARIATIONS IN THE TOP COMPRESSION FIBRE

Figures 4.7 and 4.8 show the strain variations along the top compression fibre of the test beams. The magnitudes of the strains represent the average strains over the 8-in. gauge panel lengths and are plotted at the middle of each panel. The figures show maximum strains at mid-span, except for beam F1, and these strains varied from about 0.004 to 0.006 at initial compression crushing. Lower strains occurred at initial crushing for the higher concrete strengths in beams F1, F2 and G1. Figures 4.7 and 4.8 show that higher strains were developed in the short span beams compared to the long span beams for

the 1-in. pitch spiral reinforcement. For the other spiral pitches, the strain values at initial compression crushing were approximately the same.

MOMENT-CURVATURE RELATIONSHIPS

Figures 4.9 and 4.10 present the moment-curvature relationships in terms of the moment ratio M/M_i versus the mid-span curvature. The mid-span curvature is the curvature developed in gauge panel five of the instrumented gauge length. The figures show that for the range $0.6 < M/M_i < 1.0$, the rate of change of slope decreases as the pitch of the spiral reinforcement increases. The moments at failure are in the range $1.03 < M/M_i < 1.14$.

Table 5.1 presents a comparison between the mid-span curvatures at the moment, M_i, producing initial compression crushing, and those at the ultimate moment, M_u. The order of magnitude of the curvatures at M_u is about three times higher than at M_i for the 1-in. and 2-in. pitch spiral confinement in the long span series D and F beams. This is also observed in beam G2. The 3-in. spiral pitch gives a constant ratio of about 2.2. The minimum ratio is nearly 2.0. This significant increase in curvatures beyond M_i shows that plastic hinges have developed at the critical mid-span sections. The larger ratios for beams G1 and G2 compared to E1 and E2 indicate that the confinement is more effective for the higher concrete strengths and amount of tension reinforcement. This effect is not shown in the long span beams.

The shape of the relationships is essentially the same for the

same values of spiral reinforcement pitch. For each value of pitch, the shape is not significantly affected by the concrete strength, the amount of tension reinforcement or the span length.

STRAINS IN THE SPIRAL REINFORCEMENT

Figures 4.11 to 4.14 show the variations of the strains in the spiral reinforcement at the gauge locations I, II and III shown in Figure 3.6. There is an initial linear increase in the spiral strains, and the small orders of magnitude indicate that the spiral reinforcement is not required to resist significant lateral strains in the concrete until initial compression crushing occurs. Near $M/M_i = 1$, there are larger increases in the spiral strains for small load increments.

Generally, only a small lateral restraint was offered at gauge locations I and II on the side of the beams. Additional confinement provided by the load bearing block at gauge location I increased the ability of the concrete to resist spalling, and since spalling did not occur on the sides of the beams, the spiral reinforcement was not required to act to its full capacity. Tension failure of the spiral reinforcement, shown in Figure 5.6, was observed at the front face of beam G2 opposite gauge location II.

Figure 4.12 shows that the yield strain of the spiral reinforcement was developed at gauge location III in beams F1, F2 and F3. The spiral reinforcement also resisted higher lateral concrete strains in series F and G beams at this location compared to series D and E beams. A greater participation by the spiral reinforcement at this location in

all beams compared to locations I and II is generally shown at all the increments of applied load.

FAILURE MODES AND CRACK PATTERNS

The properties of all the beams showed that the beams were over-reinforced in tension according to the ACI Code (5) requirements, although an attempt had been made to provide balanced design conditions in series D and E beams.

Once initial compression crushing occurred, the confined concrete compression zone had to resist the compressive stresses due to the applied load. The behaviour and type of failure of the beams at ultimate load were dependent on the ability of the spiral reinforcement to resist the lateral concrete strains, the ability of the tension reinforcement to undergo further strain, and the shear resistance of the beams.

The concrete compression zone spalled in varying degrees for the different spiral pitches. Figure 5.1 shows that the spalling did not cause any removal of the concrete bound by the 1-in. pitch spiral reinforcement. Figure 5.2 shows the spalling in beam D1. Beams D1, F1 and G1 failed by fracture of the tension reinforcement. Figure 5.3 shows the failure in shear of beam E1. An examination of beam E1 after failure revealed that two wires in the lower outside tension cable had fractured.

Concrete spalled from between the loops of the 2-in. and 3-in. pitch spiral reinforcement. Figures 5.4 and 5.5 show how the concrete arched between the spiral loops in beam D2, and to a greater extent in beam F3. The arching was significant in beam D2 which had the lowest

concrete strength for the beams with the 2-in. pitch spirals, and which finally failed in compression. For beams E2 and F2, the arching maintained the compressive resistance and tension failures resulted. Beam G2 failed in a shear-compression manner shown in Figure 5.7. An evaluation of strain in the tension reinforcement of beams D2 and G2 indicated yielding had occurred.

Beams D3 and E3 failed in compression, and beams F3 and G3 in a shear-compression manner. Figures 5.5 and 5.8 show the failures of beams F3 and E3. Beam D3 failed when a vertical crack, extending from an inclined shear crack, penetrated the confined concrete zone from below. The three inch spiral pitch was too large to prevent inclined cracks from penetrating the confined concrete zone, but it provided sufficient confinement to permit large deformations to occur before ultimate failure.

The crack patterns developed from flexural cracks which extended perpendicularly from the tension fibres, then inclined towards the point of load application. Figure 5.9 shows how the inclined cracks penetrated to the base of the spiral reinforcement in beam F2. For increased load, initial compression crushing commenced near the load bearing block, and spalling developed along the extreme compression fibres away from the bearing block. Extensive inclined cracking occurred in series E and G beams.

COMPARISONS WITH PREVIOUS TESTS

The increased deformation capacity obtained by confining the

compressed concrete zone is evident when a comparison of the present tests is made with the tests reported by Belke (3). A summary of these test results without confinement was presented in Table 2.2. A summary of the present test results is presented in Table 5.2. The comparisons which follow are based on considerations of concrete strengths and amounts of tension reinforcement.

Comparing beams D1 and 2A, the 1-in. pitch spiral confinement in beam D1 produced an increased moment of resistance, and a deflection capacity about three times higher than that in beam 2A. Beam D1 failed in tension and beam 2A in compression. Beam F3 compared to beam 3A shows a similar result except that both beams exhibit compression type failures. It is important to note that although beam F3 failed in a shear-compression manner, the confinement permitted a very much larger deformation capacity. Beam F1 has a deflection capacity about three times higher than beam 6A, although beam 6A had a concrete strength of over 1000 psi. in excess of beam F1. Beam F1 failed in tension compared to the compression failure of beam 6A. For the short span beams, beam E2 had a higher ultimate moment capacity, and the deflection capacity was about twice that of beam 2B. Beam E2 exhibits a tension failure compared to a compression failure in beam 2B. Beams G3 and 3B show similar results to beams E2 and 2B except that both failed in a compression manner.

CONFINED CONCRETE COMPRESSION ZONE

The comparisons show that the deformation capacity of the beams reported by Belke (3) was limited by the deformations which could occur

in the concrete compression zone. The prestressed beams with confined compressed concrete develop an increased ductility which permits a significant increase in the deflections, and hence rotation capacity, at the critical sections of maximum moment. The most important aspect is that if sufficient confinement is provided, i.e. by 1-in. or 2-in. pitch spiral reinforcement in this case, then tension failures will result in beams which are normally over-reinforced. The ultimate moment can be maintained over a relatively large deflection or curvature range. Thus, the confinement contributes to significant inelastic behaviour in a structural element which does not normally possess this type of behaviour. Such a characteristic is essential before a true limit analysis procedure can be applied to the design of prestressed concrete beams.

TABLE 5.1

A COMPARISON OF MID-SPAN CURVATURES

Beam	ψ_i Observed Mid-Span Curvature at $M/M_i = 1.0$ ($\times 10^{-5}$ Radians/in.)	ψ_u Observed Mid-Span Curvature at M_u ($\times 10^{-5}$ Radians/in.)	Ratio $\frac{\psi_u}{\psi_i}$
D1	112	370*	3.3
D2	136	408	3.0
D3	118	254	2.2
E1	188	350*	1.8
E2	114	234	2.0
E3	118	274	2.3
F1	92	320	3.5
F2	110	356	3.0
F3	110	246	2.2
G1	162	424	2.6
G2	108	327	3.0
G3	112	244	2.2

* The shape of the moment-curvature relationship was estimated from the load-deflection relationship near M_u for these beams. The curvatures represent minimum values.

TABLE 5.2

A SUMMARY OF THE TEST RESULTS

Beam	Span	f_c' (psi)	A_s (in^2)	$p = \frac{A_s}{bd}$	Effective Prestress (ksi)	Type of Failure	Observed M_u (kip-ft)	Observed M_i (kip-ft)	Observed M_{CR} (kip-ft)	P_u (approx) kip	Δ_{MAX} (approx) (ins)
D1	10'-0"	3470	0.3468	0.00578	131	TENSION	71.2	62.5	36.8	28.5	3.50
D2	10'-0"	3880	0.3468	0.00578	135	COMPRESSION	68.2	65.0	26.0	27.3	2.34
D3	10'-0"	3920	0.3468	0.00578	135	COMPRESSION	66.2	62.5	32.5	26.5	2.84
E1	5'-0"	3720	0.3468	0.00578	132	SHEAR	72.2	67.5	29.7	57.7	1.26
E2	5'-0"	4330	0.3468	0.00578	138	TENSION	76.3	67.5	34.4	61.0	0.90
E3	5'-0"	3540	0.3468	0.00578	134	COMPRESSION	71.2	62.5	31.9	57.0	0.80
F1	10'-0"	5340	0.4624	0.00770	144	TENSION	93.5	85.0	37.4	37.4	3.08
F2	10'-0"	5120	0.4624	0.00770	129	TENSION	94.0	82.5	36.5	37.6	3.33
F3	10'-0"	3550	0.4624	0.00770	127	SHEAR-COMPR	72.0	70.0	34.3	28.8	2.78
G1	5'-0"	5310	0.4624	0.00770	149	TENSION	108.2	95.0	43.7	86.5	1.36
G2	5'-0"	4740	0.4624	0.00770	132	SHEAR-COMPR	93.1	82.5	35.5	74.5	1.90
G3	5'-0"	3700	0.4624	0.00770	135	SHEAR-COMPR	83.7	74.8	34.4	67.0	0.79

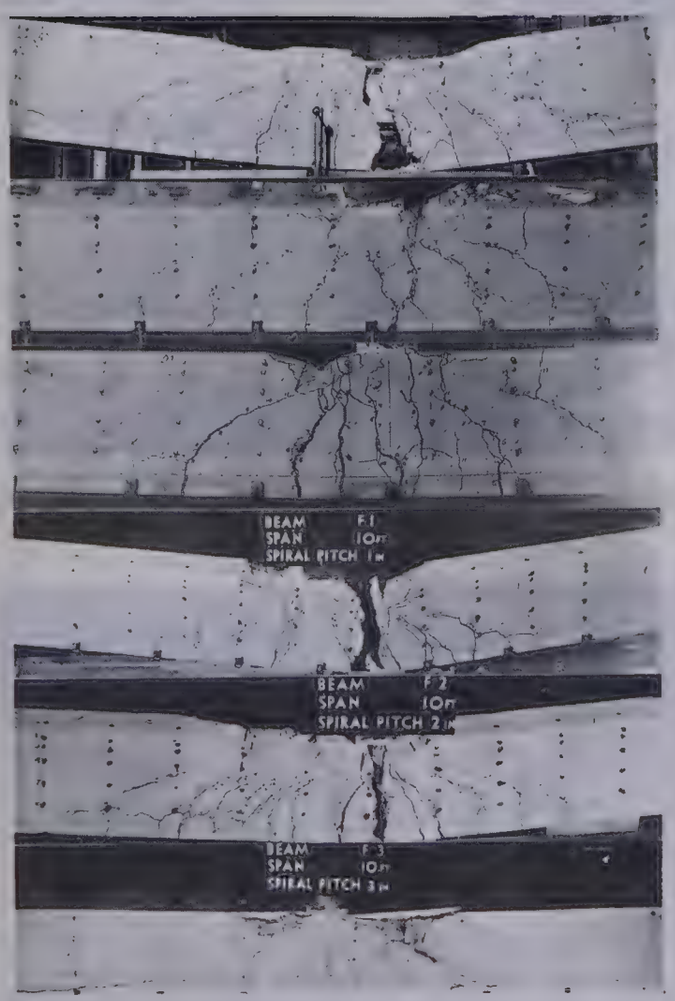

Beam D1
Span 10ft.
Spiral Pitch 1in.

Beam D2
Span 10ft.
Spiral Pitch 2in.

Beam D3
Span 10ft.
Spiral Pitch 3in.

Beam F1
Span 10ft.
Spiral Pitch 1in.

Beam F2
Span 10ft.
Spiral Pitch 2in.

Beam F3
Span 10ft.
Spiral Pitch 3in.

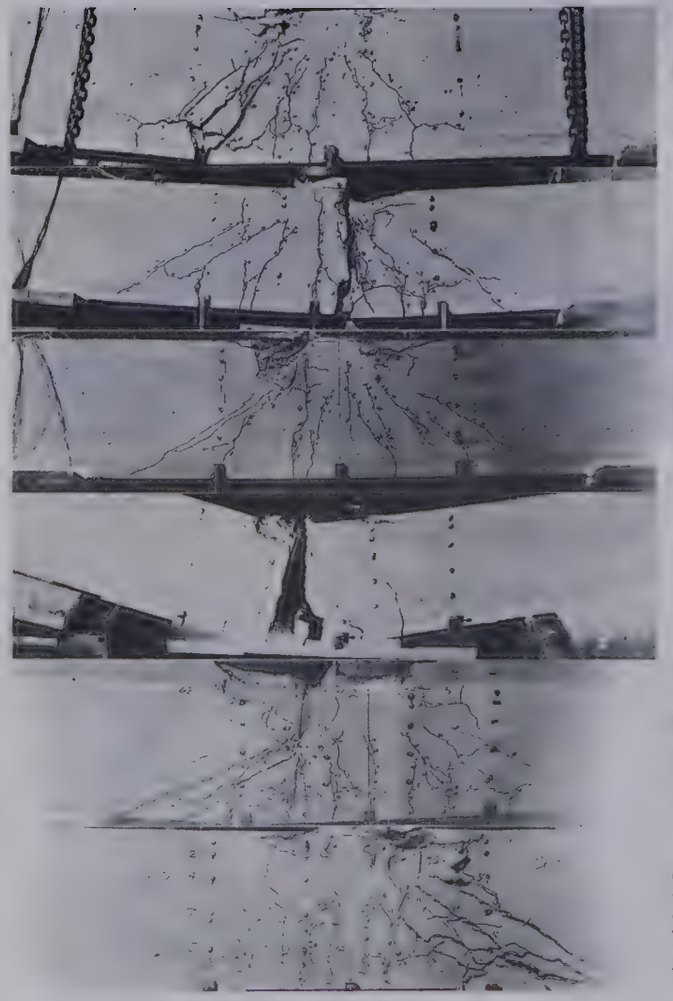

Beam E1
Span 5ft.
Spiral Pitch 1in.

Beam E2
Span 5ft.
Spiral Pitch 2in.

Beam E3
Span 5ft.
Spiral Pitch 3in.

Beam G1
Span 5ft.
Spiral Pitch 1in.

Beam G2
Span 5ft.
Spiral Pitch 2in.

Beam G3
Span 5ft.
Spiral Pitch 3in.

FIGURE 5.1: FAILURE MODES OF SERIES 'D', 'E', 'F', AND 'G' BEAMS

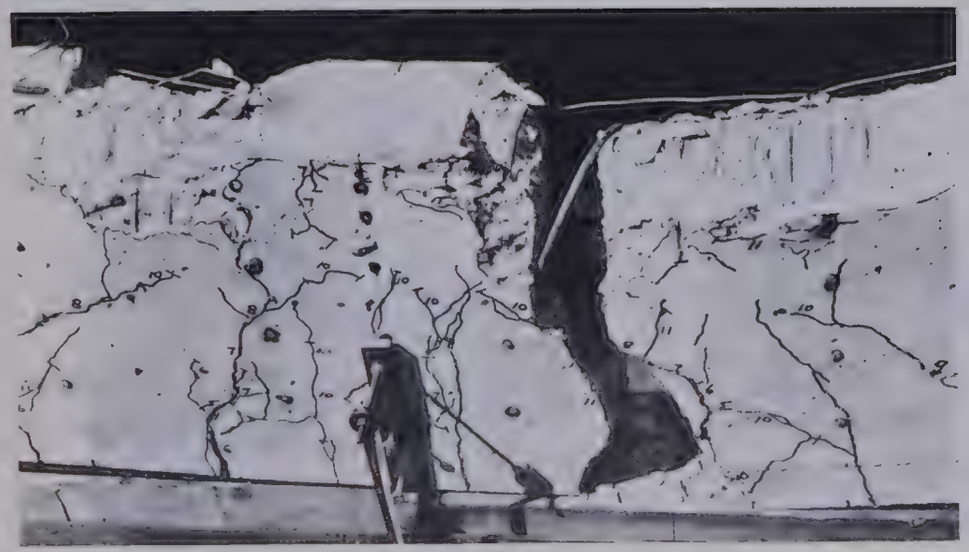

FIGURE 5.2: SPALLING AT THE COMPRESSION ZONE IN BEAM D1

FIGURE 5.3: SHEAR CRACKS PENETRATE THE COMPRESSION ZONE IN BEAM E1

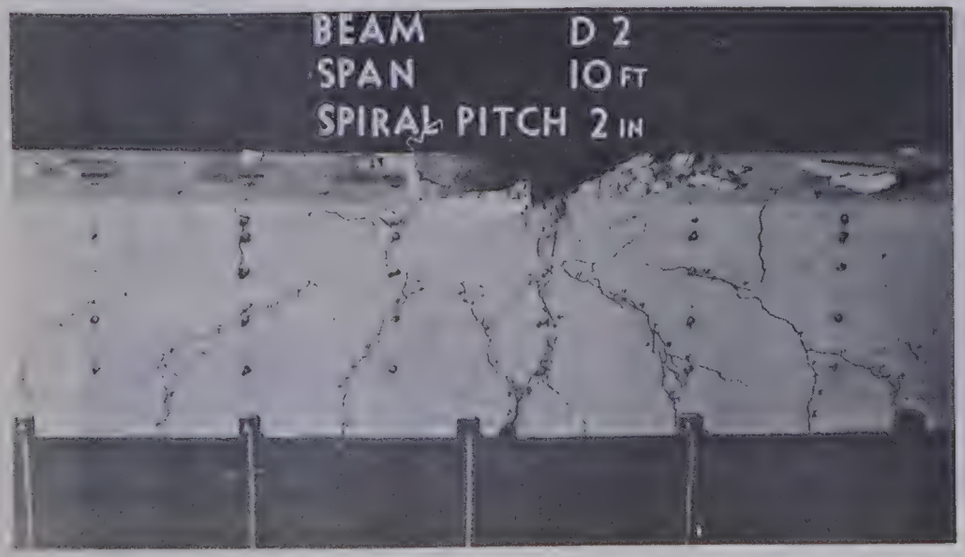

FIGURE 5.4: ARCHING BETWEEN THE SPIRAL LOOPS IN BEAM D2

FIGURE 5.5: ARCHING BETWEEN THE SPIRAL LOOPS IN BEAM F3

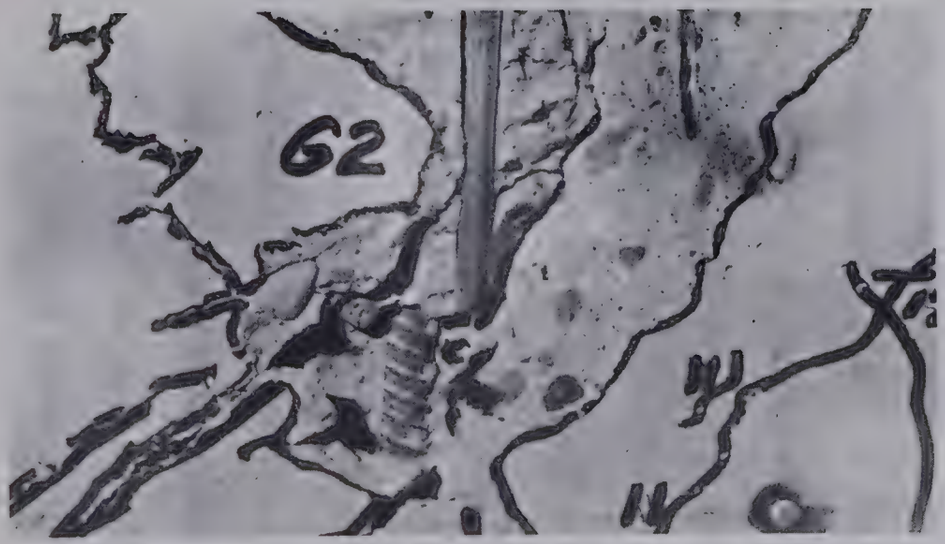

FIGURE 5.6: TENSION FAILURE OF THE SPIRAL STEEL IN BEAM G2

FIGURE 5.7: SHEAR CRACKS AND RUPTURE OF THE COMPRESSION ZONE IN BEAM G2

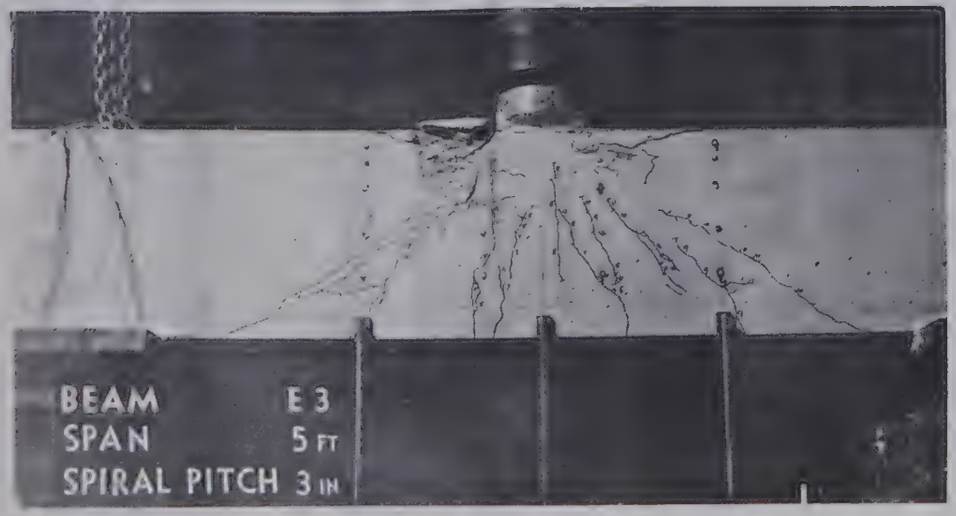

FIGURE 5.8: COMPRESSION FAILURE IN BEAM E3

FIGURE 5.9: CRACK PATTERNS AND INITIAL CRUSHING IN BEAM F2

CHAPTER VI

SUMMARY, CONCLUSIONS AND RECOMMENDATIONS

The behaviour of a series of prestressed concrete beams with confined compressed concrete has been presented in terms of their measured load-deflection relationships and derived moment-curvature relationships. The effect of the degree of confinement on the behaviour characteristics and failure modes has been discussed for beams which had varying amounts of tension reinforcement, varying span lengths, nominal variations in concrete strength, and small variations in the effective prestress levels.

Confining the compressed concrete zone increased the deformation capacity of the prestressed beams. The confinement kept the bulk of the compression zone intact when initial crushing occurred at the extreme compression fibres. The confined concrete zone permitted the prestressed concrete beams to resist a moment, at least equal to the maximum moment, for a large range of mid-span curvature regardless of the final mode of failure. The confinement provided these prestressed beams with the ability to develop plastic hinges at critical sections of maximum moment. Where sufficient confinement had been provided, tension failures were developed in prestressed concrete beams which, according to the ACI Code requirements (5), were normally over-reinforced.

The results obtained in this experimental investigation lead to the following conclusions:-

(1) For similar concrete strengths, amount of tension reinforcement, and span length; to ensure tension failures in prestressed concrete beams which have large amounts of tension reinforcement

the degree of confinement must be sufficient so that yield strains are developed in the tension reinforcement.

(2) For similar concrete strengths, amount of tension reinforcement and degree of confinement; a change in the failure mode due to a reduced span length depended on the shear resistance of the beam. If the concrete strength and web reinforcement were sufficient to develop the required shear resistance, then the failure mode depended on the amount of confinement.

(3) For similar concrete strengths, degree of confinement, and span length; a larger amount of tension reinforcement did not significantly affect the behaviour and ultimate curvature, however, it did increase the resisting moment capacity.

Increased curvatures were developed using spiral-wound reinforcement to confine the concrete compression zones of prestressed concrete beams. This method of confinement had been reported (8) as the most economical on the basis of weight of steel per unit length of the confined zone. Alternatively, it might be possible to obtain increased curvatures by using compression reinforcement. It is recommended that the next series of tests should include prestressed beams having compression reinforcement to determine if sufficient deformation capacity can be developed to permit plastic hinges to form at critical sections. In preliminary tests, the amount of compression reinforcement should be equal to the amount of spiral reinforcement (by weight) used in the present tests.

Future tests could be extended to include prestressed concrete

beams continuous over two spans with confined compressed concrete at the critical sections within the spans and at the negative moment region over the central support.

LIST OF REFERENCES

1. Warwaruk, J., Sozen, M.A., and Siess, C.P., "Strength and Behaviour in Flexure of Prestressed Concrete Beams", University of Illinois, Experimental Station Bulletin No. 464, August 1962.

2. Raffa, G., "Deformation Characteristics of Pretensioned Concrete Beams in Flexure", M.Sc. Thesis, University of Alberta, October 1964.

3. Belke, T., "Deformation Characteristics of Pretensioned Concrete Beams Subject to Bending and Shear", M.Sc. Thesis, University of Alberta, May 1965.

4. Ward, R.L., "Pretensioned Beams with Confined Compressed Concrete", M.Sc. Thesis, University of Alberta, April 1966.

5. ACI STANDARD 318-63, "Building Code Requirements for Reinforced Concrete", June 1963.

6. Sherbourne, A.N., and Parameswar, H.C., "Limit Analysis of Continuous Prestressed Beams", Proceedings ASCE, Vol. 94, ST1, January 1968, p. 19.

7. Bennett, E.W., Cooke, N., and Naughton, L.P., "Deformation of Continuous Prestressed Concrete Beams and Its Effect on the Ultimate Load", Proceedings ICE, Vol. 37, May 1967, p. 57.

8. Base, G.D., and Read, J.B., "Effectiveness of Helical Binding in the Compression Zone of Concrete Beams", Journal ACI, July 1965, p. 763.

NOTATION

A_s = area of prestressed tendons

b = width of compression face of test beam

d = distance from extreme compression fibre to centroid of the prestressing force

E_c = modulus of elasticity of concrete

f_c' = compressive strength of concrete

f_r = modulus of rupture of concrete

kd = distance from extreme compression fibre to the neutral axis

M = bending moment due to externally applied load

M_{CR} = net flexural cracking moment

M_i = bending moment at observed initial compression crushing at the extreme compression fibre

M_u = ultimate resisting moment

p = A_s/bd ratio of prestressing steel

P_u = ultimate applied load

Δ_{MAX} = mid-span deflection at P_u

ε_c = strain in the extreme concrete compression fibre

ε_{SPY} = yield strain of the spiral reinforcement

ψ = ε_c/kd = curvature

ψ_i = observed mid-span curvature at M_i

ψ_u = observed mid-span curvature at M_u

APPENDIX

MATERIALS, FABRICATION, PRESTRESS LOSS AND LOADING APPARATUS

MATERIALS

Cement

Type III, high early strength, Portland Cement was used for the fabrication of all the beams.

Aggregate

The sand used for the fine aggregate had a fineness modulus of 2.53 and an average moisture content of about 4%. The coarse aggregate was 3/8-in. maximum size pea gravel. Sieve analyses for the aggregates are presented in Tables A.1 and A.2.

Concrete Mixes

The concrete mix design (by weight) used for the fabrication of the test beams was:-

(1)	cement	1.0,
(2)	sand	3.1,
(3)	coarse aggregate	2.2.

By varying the water/cement ratio for individual mixes, concrete strengths ranging from 3500 psi to 4330 psi were obtained. At a later stage in the test program the concrete mix design was adjusted to:-

(1) cement 1.0,

(2) sand 2.5,

(3) coarse aggregate 1.7.

Concrete strengths between 4740 psi and 5340 psi were obtained. The concrete mix proportions, the water/cement ratio, the slump, the compressive and tensile strengths, and the age at test, are listed for each test beam in Table A.3. The compressive and tensile strengths were determined from tests on 6-in. by 12-in. concrete control cylinders. The modulus of rupture and modulus of elasticity were calculated using (1):-

$$f_r = \frac{3000}{3 + \frac{12000}{f_c'}} \qquad (2)$$

$$E_c = \frac{30 \times 10^6}{6 + \frac{10000}{f_c'}} \qquad (3)$$

These properties are presented in Table A.4.

Prestressing Strand

The prestressing strand used in the fabrication of the test beams was 250K grade, 7-wire strand, 5/16-in. nominal diameter, and complied with A.S.T.M. A-416 specifications. The stress-strain diagram is presented in Figure A.1.

Shear Reinforcement

The shear stirrups were either #2 plain bent bars or #3 deformed bent bars. The yield strengths were 42 ksi and 55 ksi respectively.

Spiral Reinforcement

6-in. outside diameter and 4-ft. long spiral reinforcement was manufactured with 1-in., 2-in., and 3-in., pitches from #2 plain bars (4). The stress-strain diagram for the as supplied condition of the #2 plain bars is shown in Figure A.2.

FABRICATION

Forms

The test beams were cast in pairs in a continuous metal form. The form was fabricated using two 12-in. steel channel sections for the removable sides, and an 18-in. channel base. To provide an overall beam depth of 14-5/8 in. the form was modified with wooden spacers placed between the side and base channel sections. End plates of 6-in. channel section were drilled to accommodate the prestress cables at the required spacing and effective beam depth. The form is shown erected between two concrete bulkheads anchored to the laboratory loading floor in Figure A.3.

Prestressing

The cables were prestressed with only the base channel in place.

The reactions for the prestressing operation were provided by the two concrete bulkheads. The cables were threaded through the spacer holes in the form end plates, and through end plates centred at the bulkheads. The plates were drilled with the appropriate spacing requirements to allow correct alignment of the cables to be maintained during the prestressing procedure. Each cable was tensioned individually with a Simplex centre hole hydraulic jack operated by a Blackhawk hand pump. The cables were gripped at the end plates with wedge-grip end anchorages. Aluminum dynamometers were used to measure the tension in the cables (2),(3),(4). These arrangements are shown in Figures A.4 and A.5. The prestressing equipment is shown in Figure A.6.

Shear Stirrups and Spiral Reinforcement

The shear stirrups were wired directly to the prestressed cables as shown in Figure A.7, and the side forms were erected and bolted in place. The spiral reinforcement was placed and wired to the shear stirrups. To keep the stirrups upright during the placement of the concrete, they were wired to a #3 reinforcing bar supported above the forms. The wires were cut and the #3 bar removed after the concrete had been placed and vibrated. The final arrangement prior to placing of the spirals and casting is shown in Figure A.3.

Casting and Curing

The concrete was mixed in a nine cubic feet capacity upright mixer. Two batches of approximately 7-1/2 cu. ft. were required to cast two beams and their control cylinders. One each of series D and E beams

were cast at a time, eg. D1 and E1, then similarly for series F and G beams. The first batch was used to cast the shorter series E or G beam and its control cylinders, with the remaining concrete being placed in the end portions of the longer D or F series beam. The second batch was placed in the centre region of the series D or F beam and used to cast its control cylinders. This procedure ensured uniformity of the concrete over the gauge length of a particular beam. The concrete was compacted using a high frequency immersion vibrator.

The test beams were covered with wet burlap and a plastic sheet, and cured for twenty-four hours, after which the forms were stripped and the wet burlap and plastic sheet replaced. After four to five days of moist curing, the burlap and plastic sheet were removed to allow the beam surface to dry out.

Six 6-in. by 12-in. control cylinders were cast for each test beam. The control cylinders were cured and stored under the same laboratory conditions as the beams. Four cylinders were used for compression tests and two for tension splitting tests. On the day of a beam test, two control cylinders were tested in compression and two in tension splitting.

Release of Prestress

Demec gauge points were positioned on the test beam gauge length and readings recorded. The location of the Demec points is shown in Figures 3.4 and 3.5. Final readings on the dynamometers were recorded and the prestressed cables were cut. A cutting torch was used to heat the cables to allow a gradual transfer of stress to the concrete. Immediately after the release of prestress, the Demec gauge point

readings were recorded. The loss of prestress force due to elastic shortening of the concrete, resulting from the transfer of stress from the cables to the concrete, was calculated from the differences in the Demec gauge readings, and is tabulated in Table A.5.

TOTAL PRESTRESS LOSSES

The total prestress losses combined those due to the elastic shortening of the concrete, and the shrinkage and creep of the concrete which occurred from the time of prestress release to the testing of the beam. The losses due to shrinkage and creep were determined from the differences between the Demec readings recorded after prestress release and those recorded as initial readings at the beginning of each beam test. The total prestress loss and effective prestress for each beam is presented in Table A.5.

LOADING APPARATUS

The single point concentrated load was applied using a 220 kip Amsler hydraulic jack. The loading frame and jack arrangement are shown in Figure A.8. An Amsler Pendulum Dynamometer was used to measure the applied loads. The facility of the built in load maintainer made it possible to keep the load at a constant level independent of creep in the test beam while under an applied load. The load was applied through a 6-in. by 6-in. bearing plate fixed to the top concrete compression fibre using Plaster of Paris. This provided an even stress distribution in the beam under the load point. The test beam was

supported by hinged and roller type supports set on concrete pedestals. The pedestals were set firm on the laboratory floor using Plaster of Paris.

TABLE A.1

SIEVE ANALYSIS OF SAND

Sieve Size	Weight Retained (gms)	% Retained	Cumulative % Retained	A.S.T.M. Standard
#4	17.5	3.0	3.0	0 - 5
#8	85.2	14.7	17.7	
#16	54.6	9.5	27.2	20 - 55
#30	60.0	10.3	37.5	
#50	208.4	35.8	73.3	70 - 90
#100	122.9	21.1	94.4	90 - 98
PAN	17.8	3.1	-	
SILT	14.4	2.5	-	
TOTAL	580.8	100.0		
FINENESS MODULUS		2.53		

TABLE A.2

SIEVE ANALYSIS OF COARSE AGGREGATE

Sieve Size	% Retained	Cumulative % Retained
3/4	0	0
3/8	5.9	5.9
#4	87.1	93.0
PAN	7.0	100.0
TOTAL	100.0	

TABLE A.3

CONCRETE CYLINDER STRENGTHS AND PROPERTIES

Beam	Cement: Sand: Gravel (by weight)	Water: Cement (by weight)	Slump (in)	Compressive Strength (psi)		Tensile Strength (psi)		Age At Test (days)	Compressive Strength (psi)	
				(1)	(2)	(1)	(2)		(5 days)	(7 days)
D1	1:3.1:2.2	0.66	5-1/2	3413	3523	274	281	22	2833	3102
D2	1:3.1:2.2	0.63	3-1/2	3855	3908	314	345	29	3307	3293
D3	1:3.1:2.2	0.54	4-1/2	3811	4032	309	-	25	3296	-
E1	1:3.1:2.2	0.59	5	3643	3802	283	287	23	3165	3519
E2	1:3.1:2.2	0.66	2-1/2	4244	4421	363	371	19	3427	3664
E3	1:3.1:2.2	0.55	4	3492	3593	367	371	18	3095	3006
F1	1:2.5:1.7	0.42	2-1/4	4188	5341	385	424	19	5146(8)	5270(8)
F2	1:2.5:1.7	0.39	2	5058	5178	380	416	23	4191	3563
F3	1:3.1:2.2	0.63	3-1/2	2706	3554	237	347	21	2440(6)	3059
G1	1:2.5:1.7	0.42	2	5213	5411	350	425	15	5341(8)	5058(8)
G2	1:2.5:1.7	0.40	3-1/2	4654	4828	347	439	21	3519	4014
G3	1:3.1:2.2	0.63	2-1/2	3608	3791	202	285	23	3183(6)	3201

TABLE A.4

CONCRETE DESIGN PROPERTIES

Beam	Compressive Strength (psi)	Tensile Strength (psi)	Modulus of Rupture (psi)	Modulus of Elasticity (psi)
D1	3470	278	464	3.38×10^6
D2	3880	330	493	3.50 "
D3	3920	309	495	3.51 "
E1	3720	285	482	3.45 "
E2	4330	367	520	3.61 "
E3	3540	369	469	3.40 "
F1	5340	405	571	3.81 "
F2	5120	398	562	3.77 "
F3	3550	292	470	3.40 "
G1	5310	388	570	3.81 "
G2	4740	393	542	3.70 "
G3	3700	244	481	3.45 "

TABLE A.5

PRESTRESS LOSSES AND EFFECTIVE PRESTRESS

Beam	Area of Reinforcement $(in)^2$	Total Prestress Force (kip)	Average Initial Prestress (ksi)	Average Elastic Shortening (ksi)	Average Creep & Shrinkage (ksi)	Total Losses (ksi)	Effective Prestress (ksi)
D1	0.3468	56.78	163.7	13.4	19.2	32.6	131.1
D2	"	58.53	168.8	12.4	21.5	33.9	134.9
D3	"	57.90	167.0	14.4	18.0	32.4	134.6
E1	"	56.78	163.7	12.2	19.3	31.5	132.2
E2	"	58.53	168.8	12.0	18.5	30.5	138.3
E3	"	57.90	167.0	15.7	17.0	32.7	134.3
F1	0.4624	78.77	170.4	12.8	13.8	26.6	143.8
F2	"	75.60	163.5	14.4	20.1	34.5	129.0
F3	"	77.04	166.6	15.4	24.0	39.4	127.2
G1	"	78.77	170.4	10.9	10.0	20.9	149.3
G2	"	75.60	163.5	13.6	18.1	31.7	131.8
G3	"	77.04	166.6	11.9	19.4	31.3	135.3

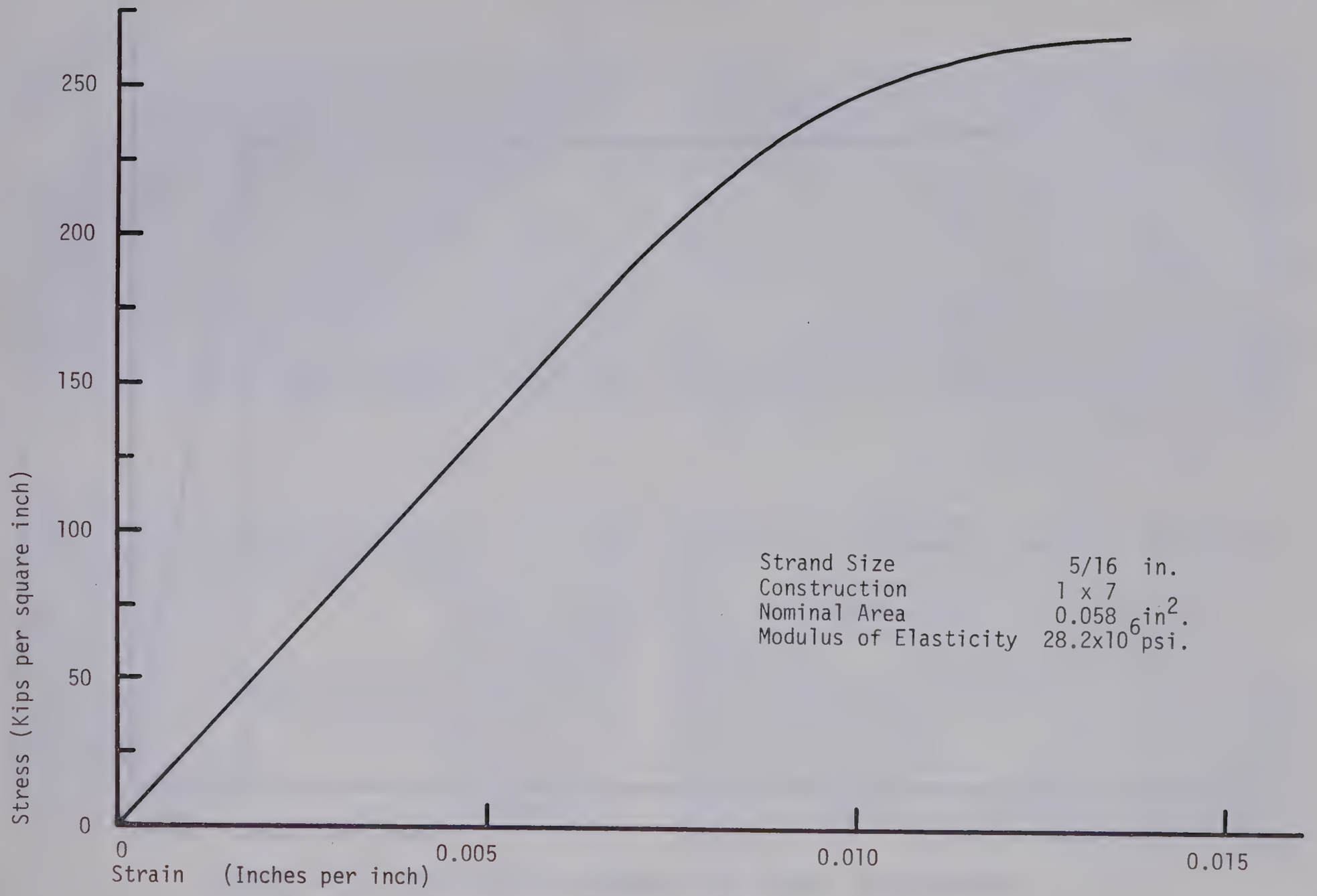

FIGURE A.1: STRESS-STRAIN DIAGRAM FOR PRESTRESSING STRAND

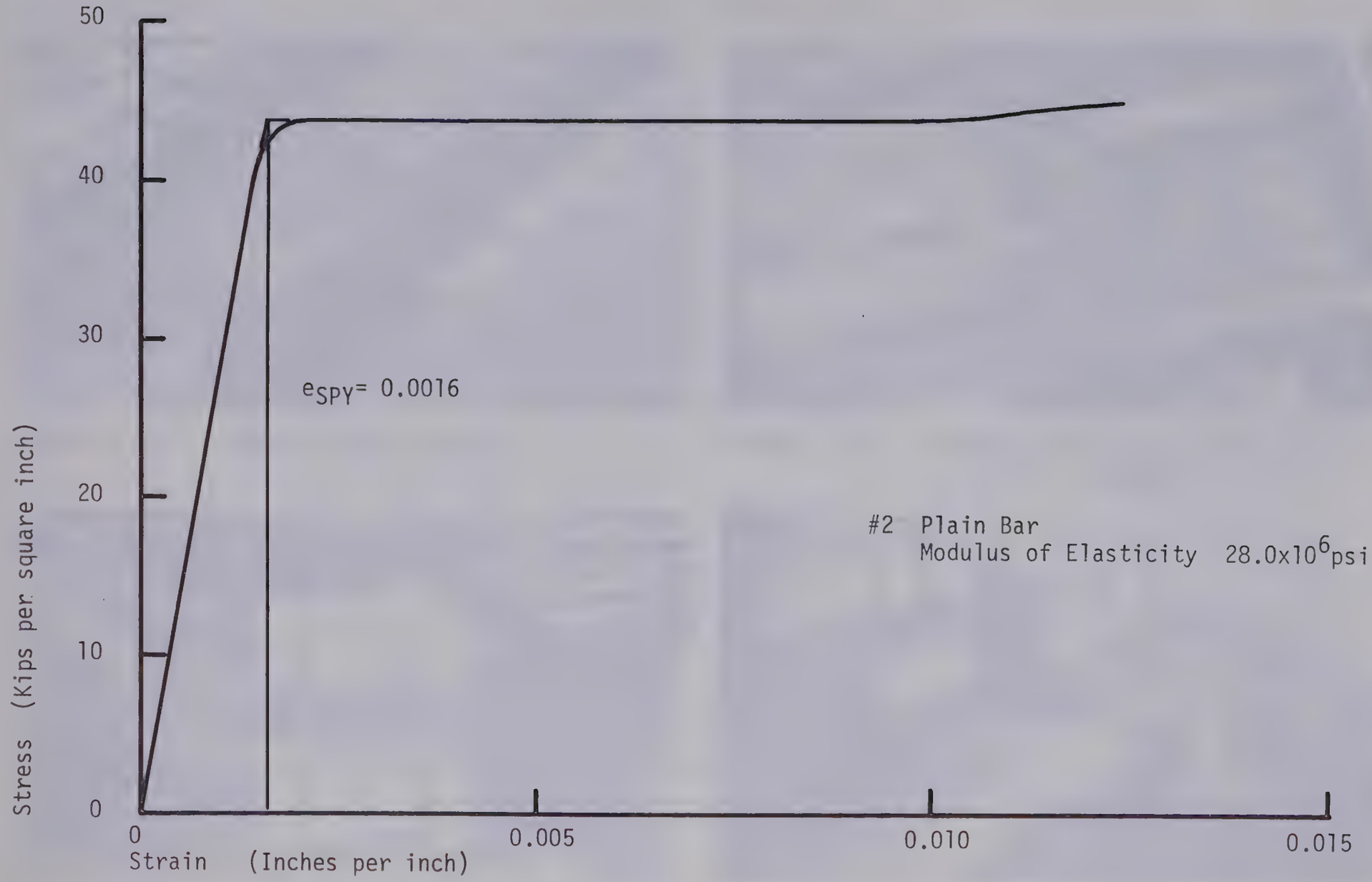

FIGURE A.2: STRESS-STRAIN DIAGRAM FOR SPIRAL REINFORCEMENT

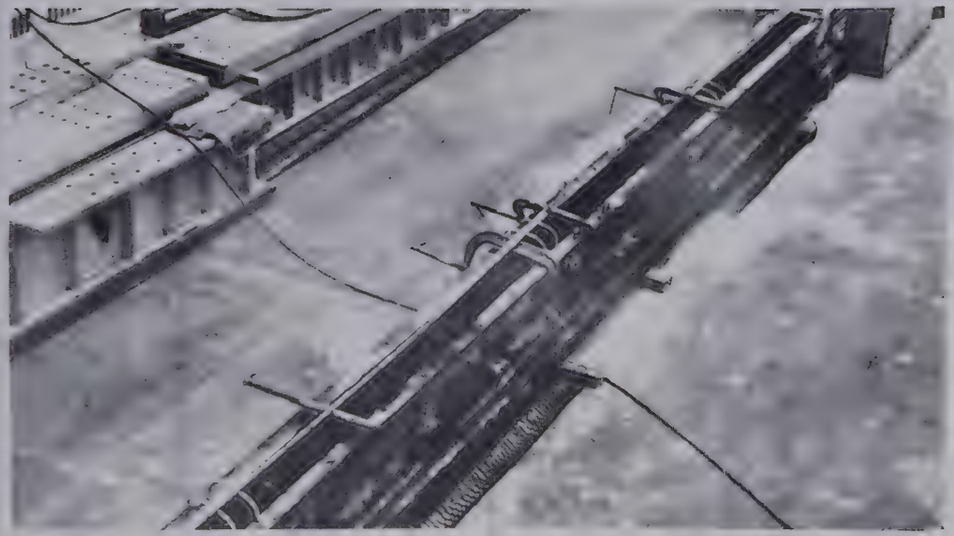

FIGURE A.3: ERECTED BEAM FORMS

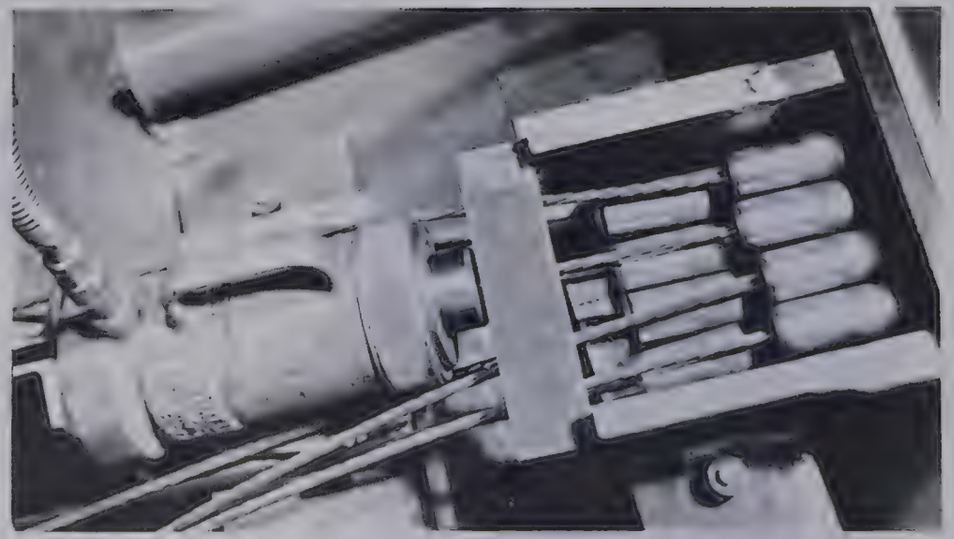

FIGURE A.4: SIMPLEX HYDRAULIC JACK AND GRIP ASSEMBLY

FIGURE A.5: ALUMINUM DYNAMOMETERS AND GRIP ASSEMBLY

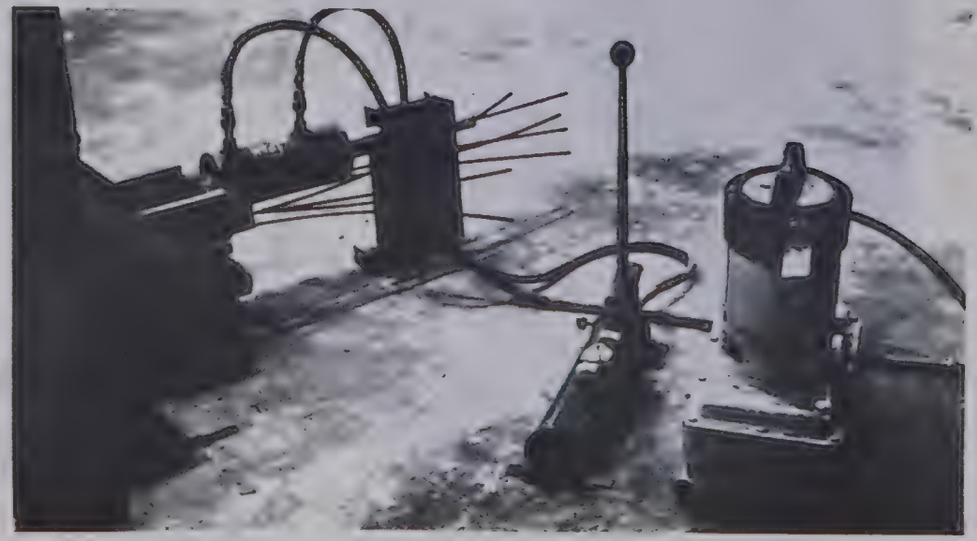

FIGURE A.6: PRESTRESSING EQUIPMENT

FIGURE A.7: SHEAR STIRRUPS WIRED TO THE PRESTRESSED CABLES

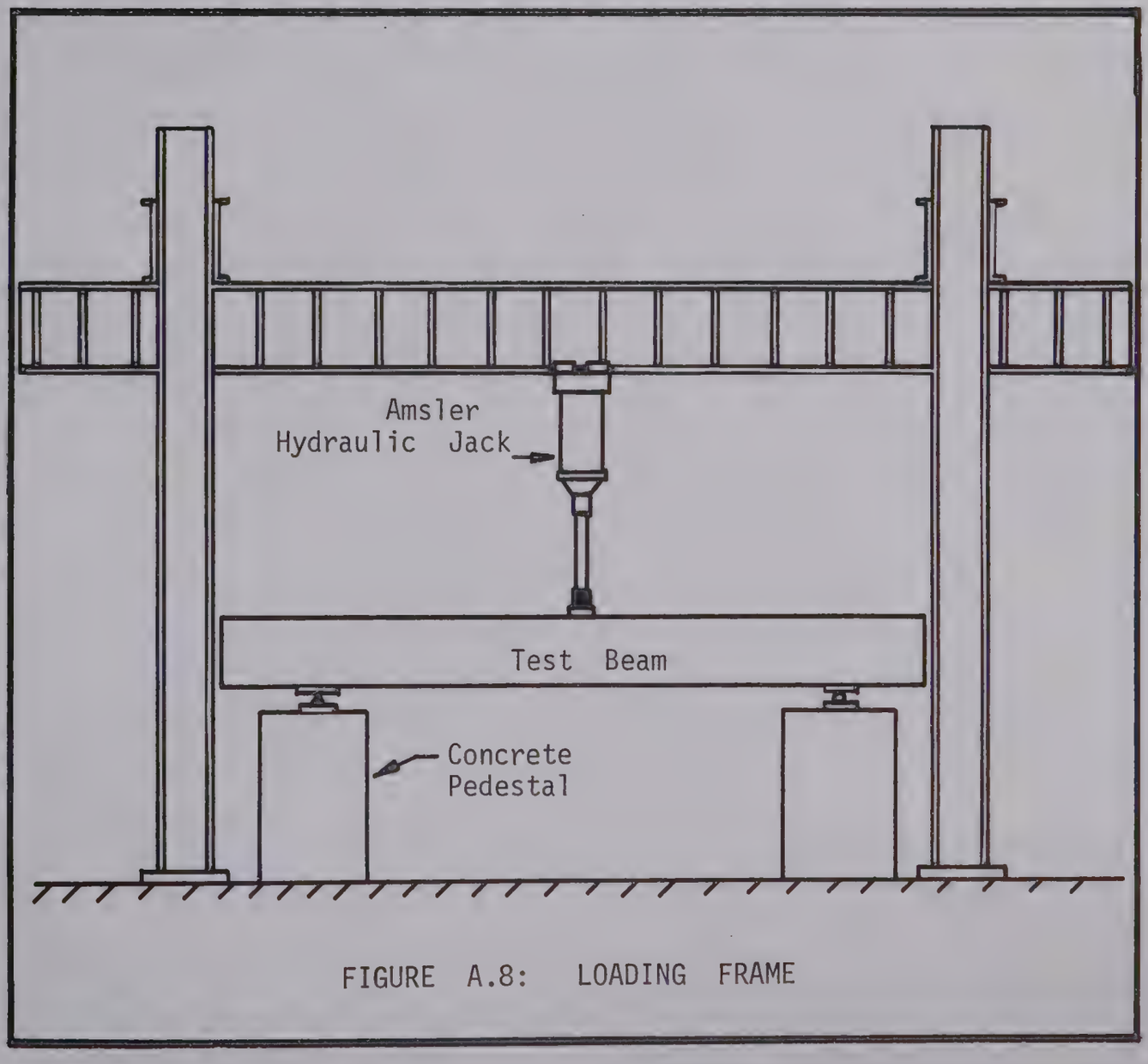

FIGURE A.8: LOADING FRAME

The University of Alberta
Printing Department
Edmonton, Alberta

B29914